Eren Dikmen

Study of Process-Induced Stress in Vitrimer Matrix Composites

FRP++
Advanced structural analysis and design using composite materials

Master Dissertation
European Master Advanced Structural Analysis and Design using Composite Materials

Work developed under the supervision of
Professor Doctor Philippe Olivier

Funded by the European Union

September 2025

DECLARATION

Name: Eren Dikmen

Email: eren.dikmen@hotmail.com **Phone number:** +33 7 74 90 46 87

Citizen Card Number: U30541331

Title of the Thesis: Study of Process-Induced Stress in Vitrimer Matrix Composites

Supervisors:

Professor Doctor Philippe Olivier

Year of Conclusion: 2025

Master Course in Advanced Structural Analysis and Design using Composite Materials

University of Toulouse III Paul Sabatier, 28/08/2025

Signature:

ACKNOWLEDGEMENTS

On sheet 2 - page 3 of the document should include:

a. the author's acknowledgements, when applicable.

b. a mention of financial support, when applicable.

Titre de la Thèse

RESUME

Cette page doit contenir le titre et le résumé de la thèse rédigée en français. À la fin de la page et dans la même langue, les mots-clés doivent être indiqués. Le résumé (y compris les mots-clés) ne doit pas dépasser une page.

MOTS-CLES: Mot-clé 1 ; Mot-clé 2 ; Mot-clé 3 ; Mot-clé 4 ; Mot-clé 5.

Dissertation Title

ABSTRACT

KEYWORDS: Vitrimer; Stress Relaxation; Bond Exchange; Thermal Characterization; Impedancemetry.

TABLE OF CONTENTS

LIST OF FIGURES

LIST OF TABLES

LIST OF ABBREVIATIONS AND SYMBOLS

Abbreviations

ACI	American Concrete Institute
CEN	European Committee for Standardization
CFRP	Carbon Fibre Reinforced Polymer
CNR	Advisory Committee on Technical Recommendations for Construction
CO_2	Carbon Dioxide

Symbols

E_a	Elastic modulus of the adhesive
ε_a	Ultimate strain of the adhesive
E_f	Elastic modulus of the CFRP laminate
ε_f	Ultimate strain of the CFRP laminate

THIS PAGE WAS INTENTIONALLY LEFT BLANK

1. INTRODUCTION

Composite materials have emerged as strong alternatives to traditional engineering materials such as metals, particularly in high-performance sectors like aeronautics and automotive industries. Precise data regarding global composite production remains limited; however, market analyses forecast an increase in the composite sector from approximately £55 billion in 2016 to nearly £87.5 billion by 2022 [1].Their physical and mechanical properties, including low density, high strength-to-weight ratio, excellent stiffness, and durability, provide significant advantages for applications where reducing weight without compromising mechanical performance is essential. These characteristics make composites highly attractive for next-generation designs, where efficiency and performance are key drivers. In aeronautics, for example, lighter structures translate directly into reduced fuel consumption and lower emissions, while in automotive manufacturing, weight reduction contributes to energy efficiency and improved vehicle dynamics. Figure 1 shows the distribution of composite applications across different industries. The largest share is in the automotive industry, accounting for more than 30% of total use, followed by aeronautics with over 20%. Civil engineering, sports and leisure , and electronics also represent notable portions of the market. Meanwhile, sectors such as shipbuilding, medical equipment, and railways contribute only marginally, highlighting that composite utilization is still concentrated in a few key industries where weight reduction and performance benefits are most critical which composites are used because of their low density.

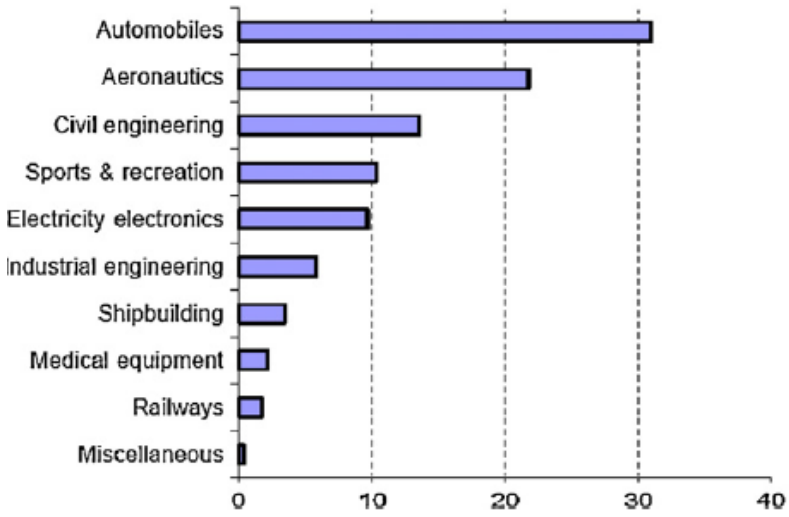

Figure 1 Application of composite materials [2]

Despite these advantages, two major challenges restrain the widespread and sustainable usage of composites. The first is their high production cost. Advanced composites, particularly carbon fiber reinforced polymers, involve complex manufacturing processes and expensive raw materials, which make them significantly more costly than conventional metals such as aluminum or steel. This cost barrier limits their use to high-value industries, preventing broader industrial applications. The second, and arguably more critical, issue is their lack of recyclability. Unlike metals, which can be melted down and reprocessed with minimal loss of properties, conventional composite materials are thermoset-based, meaning that once they are cured, their crosslinked structure cannot be re-melted or reshaped. This irreversible network of traditional thermoset matrix makes recycling nearly impossible with current methods.

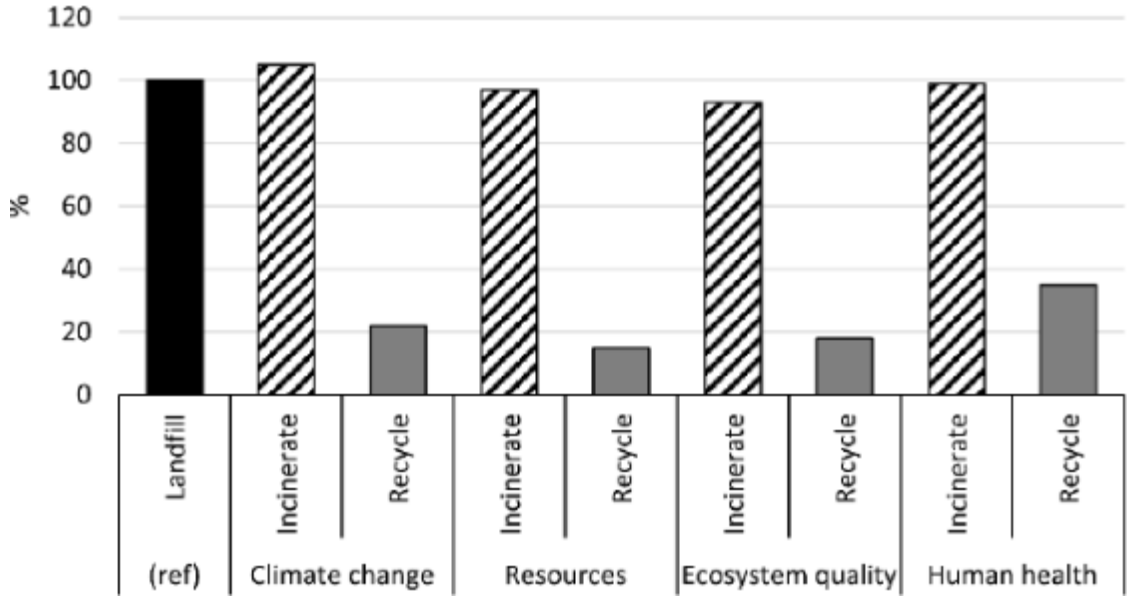

Figure 2 The impact comparison of landfill disposal, incineration and recycling [2]

As a result, composite waste management has become a growing environmental and industrial concern. At the end of their life cycle, composite parts are typically disposed of through landfilling or incineration. Landfilling not only consumes space but also poses long-term environmental risks, while incineration releases harmful emissions and wastes the embedded energy and resources used in their production as can be seen from Figure 1. Both methods are not appropriate for the principles of sustainability and make it impossible to integrate composites into a circular economy, where materials are reused, reprocessed, or reintegrated into production cycles. The increasing demand for composites in large-scale industries only shows the urgency of finding solutions to this problem, as the accumulation of non-recyclable composite waste continues to rise.

For aerospace industry, The International Air Transport Association (IATA) has projected the retirement of approximately 11,000 aircraft over the next decade [3]. This accelerated decommissioning further emphasizes the urgency of addressing aircraft recycling and end-of-life management, especially when the proportion of composite materials used in modern aircraft has risen significantly in recent decades as mentioned. Meanwhile in automative sector, composites have traditionally been employed in high-performance sports cars, where lightweight design directly corresponds to superior performance. However, recent developments in electric propulsion and autonomous driving technologies have created a broader demand for lightweight solutions. At the same time, the high-volume nature of automotive production has introduced new challenges related to end-of-life (EoL) management, as the large-scale use of composites requires efficient recycling pathways. Similar to aerospace applications, composite waste in the automotive industry is significant, with estimates suggesting that 20–40% of raw carbon fiber material may be scrapped during component manufacturing [4]. Broader adoption of CFRPs (carbon fiber reinforced polymers) in vehicle structures has the potential to reduce vehicle weight by up to 30% compared to conventional materials, directly supporting fuel efficiency targets [5]. However, the European Union regulations for instance, requires a car to be 85% recyclable which limits the usage of unrecyclable composites with traditional thermoset matrix.

Table 1 Composites recycling processes [6]

Process	Type	Input	Product/Wastes
Pyrolysis	2,3,4	In-house or post-consumer SMC	Fuel gas, oil, inorganic soil
Pyrolysis and Milling	2,3,4	SMC	Fuel gas, oil, inorganic soil
Pyrolysis	2,3,4	Polyurethane foams	Gas, oil, solid waste
Hydrolysis	4	Foams, RIM resin and elastomers	Monomers of the input material
Fluidized bed combustion	4	RIM	Heat, solid and gaseous wastes
Rotary kiln combustion	4	RIM	Heat, solid and gaseous wastes
Incineration	4	ASR “pellets”, fuel supplement	Heat, solid and gaseous wastes
Incineration	4	Auto battery plastic scraps, ASR	Heat, solid and gaseous wastes

Compression molding	2	Short or long fiber thermoplastic composites	Flake for use in compression molding
Injection molding	2	Short or long fiber thermoplastic composites	Injection molding pellets

Table 1 provides a comprehensive summary of some part of the recycling technologies currently available for thermoset and thermoplastic matrix composite materials, classified according to the four main categories of recycling: primary, secondary, tertiary, and quaternary. As known, monolithic thermoplastics are generally more straightforward to recycle due to their reprocessable nature containing semi-crystalline and amorphous natures instead of a network structure. By contrast, composite materials present significant challenges, primarily owing to the presence of reinforcing phases and the prevalence of thermosetting matrices. These characteristics complicate reprocessing and often limit composites to more energy- or chemically-intensive recycling pathways.

Primary recycling (type 1), which involves reprocessing into the same or similar applications, is not feasible for traditional composite matrix. Instead, most existing methods fall under secondary recycling (type 2 in the table), where regrinding techniques such as those applied to RIM, phenolic, or SMC materials yield ground particles that are subsequently reused as fillers or in compression and injection molding processes. While these approaches do extend the material's lifecycle, they typically result in downcycling, as the recycled material is of lower performance compared to the inital part.

Tertiary recycling processes (type 3), such as hydrolysis and pyrolysis, are increasingly explored for thermoset composites. Hydrolysis enables recovery of monomers from foams and elastomers, while pyrolysis processes produce gas, oil, and solid residues from inputs such as polyurethane foams, SMC, or auto-shredder residues. These methods offer some potential for recovering value from waste, but are energy-intensive and often associated with by-products that require careful handling,

Finally, quaternary recycling refers to energy recovery routes such as incineration and fluidized bed combustion. Although these processes can provide useful energy outputs and reduce landfill burden, they do not contribute to material circularity and still generate significant solid and gaseous wastes.

So the result from the table might be that the majority of recycling technologies for traditional composites remain focused on either secondary recycling or quaternary recovery, with only limited progress toward achieving a truly circular recycling model. This aligns with the observation that for effective recycling, not only must suitable methods and material exist, but

the entire chain of collection, reprocessing, and reintegration into valuable products must function without disruption. Failure at any stage results in the loss of recycling potential. Consequently, while recycling routes for composites are available, they are predominantly downcycling or energy recovery strategies, and genuine closed-loop recycling remains an ongoing technical and industrial challenge [7].

As a result, recyclability remains one of the most critical challenges in composite production and end-use, particularly in sectors such as aeronautics, wind energy, and the automotive industry, each of which is subject to distinct recycling regulations. Conventional thermoset matrix polymers are inherently difficult to recycle, and the current recycling methodologies often fail to restore equivalent mechanical performance while simultaneously generating significant amounts of secondary waste. To address these limitations, several research directions are possible: (i) the development of novel recycling methodologies for traditional thermoset-based composites, (ii) the exploration of alternative design strategies aimed at reducing overall composite usage in industry, and (iii) the pursuit of innovative polymer matrices that combine recyclability with high-performance characteristics. In this study, third approach is adopted, focusing on a recyclable polymer matrice called “vitrimers” such as thermoplastics which while retaining mechanical properties comparable to those of traditional thermosets.

1.1. Motivation

The primary motivation of this study lies in addressing one of the most pressing challenges associated with composite materials: as mentioned, their lack of recyclability. While composites are increasingly adopted across industries such as aeronautics, wind energy, and automotive engineering due to their high strength-to-weight ratio and excellent mechanical performance, their conventional thermoset matrices present a fundamental block to sustainability and recycling. Thermoset polymers, once cross-linked, cannot be reprocessed or remolded without significant decomposition in properties. Consequently, the end-of-life (EoL) management of thermoset-based composites is limited to disposal or downcycling, both of which are environmentally unsustainable and economically inefficient. This issue is particularly critical in industries that rely heavily on composite materials but are simultaneously under growing pressure to comply with strict sustainability regulations and circular economy principles.

In response to these challenges, the search for recyclable composite matrices has become an urgent research direction. Thermoplastics have been proposed as an alternative, given their inherent reprocessability; however, they often fall short of delivering the same mechanical and thermal stability required in demanding engineering applications. In recent years, vitrimers have emerged as a promising class of polymer matrices. Introduced only in the past decade, vitrimers combine the strong network structure of thermosets with the dynamic bond exchange mechanisms that enable reprocessing, repair, and stress relaxation. This unique combination of properties positions vitrimers as potential alternatives for sustainable composite technologies.
The central motivation of this thesis, therefore, is to explore vitrimer as an alternative recyclable matrix for high-performance composites. The study aims to provide an initial characterization of vitrimer matrices and vitrimer-based composites to evaluate their potential to meet industrial requirements. While vitrimers offer an exciting pathway towards reconciling performance with recyclability, their relatively recent discovery means that additional research is still required before they can be widely used. Their mechanical, thermal, and processing behaviours must be systematically compared to established thermoset systems. Ultimately, the motivation is to advance towards a sustainable composite solution that aligns with both the performance demands of advanced industries and the global imperative of environmental responsibility.

1.2. Objectives

The objective of this study is to investigate how process-induced stresses in vitrimer-based composites can be relaxed when the material is exposed to temperatures that activate dynamic bond exchange mechanism. By doing so, this work aims to contribute to the broader understanding of stress relaxation and recyclability mechanisms in vitrimer matrix composites, supporting their potential use as sustainable alternatives to conventional thermoset matrices.

To achieve this aim, the vitrimer matrix will first be thermally characterized by Differential Scanning Calorimetry (DSC), Dynamic Mechanical Analysis (DMA), and Thermomechanical Analysis (TMA) to determine its glass transition temperature, especially the secondary peak which indicates the bond exchange and the coefficient of thermal expansion. Following this, vitrimer matrix carbon fiber-reinforced composite laminates with varying dimensions and ply orientations will be fabricated by hand lay-up for different tests, vacuum bagged under different systems and cured using the same curing cycle which was studied and used for vitrimer matrix composites before. These composites will then undergo thermal analysis by DSC and DMA to

evaluate their behaviour after curing, while their microstructure will be investigated using numerical microscopy to assess void content and overall quality.

In addition, selected composite samples will be analysed by impedancemetry tests to identify critical points on the vitrimer curing curve depending on the values of impedance and tangent alpha, providing information about the phenomena related to dynamic bond exchange and strengthening the argument for vitrimer recyclability.

Finally, stress relaxation tests will be performed by subjecting curved laminates to a secondary curing cycle while noting the out of plane deformation, where reductions in curvature will be used as direct evidence of stress release depending on dynamic bond exchange.

1.3.Structure

?

THIS PAGE WAS INTENTIONALLY LEFT BLANK

2. LITERATURE REVIEW

2.1. Definition and Characteristics of Vitrimers

Since vitrimers exhibit properties characteristic of both thermosets and thermoplastics, it is essential to first provide a brief overview of these two polymer classes. This foundational understanding will help to clarify the unique structural features and defining characteristics of vitrimers. Most generally, in the context of composite materials, thermoplastic matrices allow repeated melting and re-shaping of the structures while thermosets offer rigidity and better mechanical properties in terms of strength and stiffness.

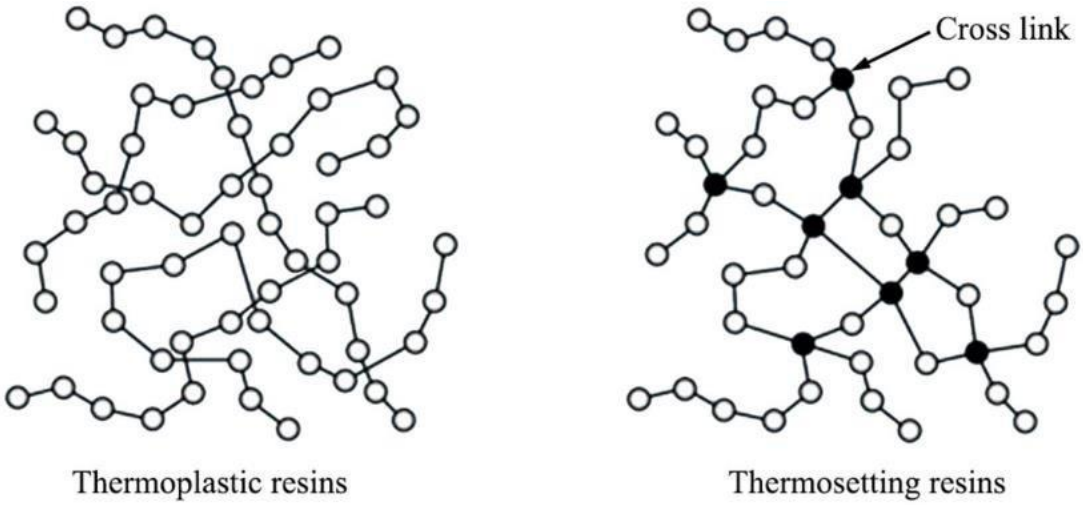

Figure 3 Molecular Structure of Thermoplastic and Thermoset Resins [1]

The primary difference in chemical structure between thermoplastic and thermoset resins is in the presence of crosslinks. Thermoplastic resins (PEEK, PEKK, PE) consist of linear or branched polymer chains without covalent bonds between them, allowing the chains to move freely past each other when heated depending on the level of semi-crystallinity which enables softening, reshaping, melting and recycling. On the other hand, thermoset resins (epoxy, polyester) undergo crosslinking when they are exposed to heat. During cure, the monomers form permanent covalent bonds which result in a three-dimensional network structure. As a result, thermosets typically exhibit greater stiffness and strength than thermoplastics as can be seen in Table 2 [2]. However, due to this crosslinked structure, thermosets cannot be remelted or recycled, and upon heating beyond a certain temperature, they decompose rather than soften or flow.

Table 2 Properties of thermoplastic and thermoset polymer matrices [3]

Matrix	Density (g/cm^3)	Failure Strain (%)	Tensile Strength (MPa)	Young's Modulus (GPa)	Glass Transition Temp. (°C)	Melting Temperature (°C)
Thermoplastic Matrices						
PP	0.89-0.92	20-400	30-40	1.1-1.6	-10 to -23	161-170
HDPE	0.94-0.96	2-130	14.5-38	0.4-1.5	-100 to -60	120-140
PS	1.04-1.06	1-2.5	25-69	4-5	100	110-135
PLA	1.21-1.25	2.5-6	21-60	0.35-3.5	45 to 60	150-162
Thermoset Matrices						
Epoxy	1.1-1.4	1-6	35-100	3-6	60 to 170	-
Polyester	1.2-1.5	4-7	40-90	2-4.5	-47 to 120	-

Table 2 highlights the key differences in mechanical and thermal properties between thermoplastic and thermoset matrices. Thermoset matrices generally exhibit higher tensile strength and stiffness compared to thermoplastics, making them more suitable for load-bearing applications. However, thermoplastics are significantly more ductile, showing greater elongation before failure, which might make them a candidate in composite applications requiring flexibility or impact resistance. Additionally, thermosets tend to have higher glass transition temperatures (Tg), reflecting better thermal stability, while thermoplastics possess defined melting points, allowing them to be reshaped and recycled through thermal processing which is not an available option for thermosets due to their crosslinked structure.

As a result, considering the structural differences mentioned between two matrix types, thermoplastic matrices offer several advantages, including unlimited shelf life, easy handling due to the absence of tackiness, and recyclability. They are also easy to repair through welding or solvent bonding, post-formable, and generally tough in mechanical performance. The notable disadvantages are being prone to creep, possibility to exhibit poor melt flow characteristics, and the need of heating above their melting point to properly wet fibers, which can complicate composite processing. On the other hand, thermoset matrices are known for their low resin viscosity, which promotes good fiber wetting. Once cured, they offer better thermal stability, are chemically resistant, and demonstrate resistance to creep. Despite these benefits, thermosets are typically brittle, non-recyclable via standard methods, and not post-formable, which limits their adaptability after curing [4].

Dynamic materials with concepts such as dynamers, covalent adaptable networks or vitrimers represent a new class of polymer networks that combine the key advantages of both thermoset

and thermoplastic matrices. Among the various research areas focused on dynamic materials, vitrimers stand out as a promising alternative, combining the desirable mechanical performance of thermosets with the ability to flow like viscous materials at elevated temperatures. Their unique properties arise from an associative exchange mechanism within the polymer network, which preserves the crosslink density and maintains a constant number of chemical bonds throughout thermal activation and reprocessing [5]. They offer the mechanical strength and thermal stability of thermosets, while also enabling reprocessability and reshaping capabilities typically associated with thermoplastics. In addition to these benefits, vitrimers introduce unique features such as self-healing, recyclability, thermoforming and stress relaxation, making them highly attractive for advanced and sustainable composite applications.

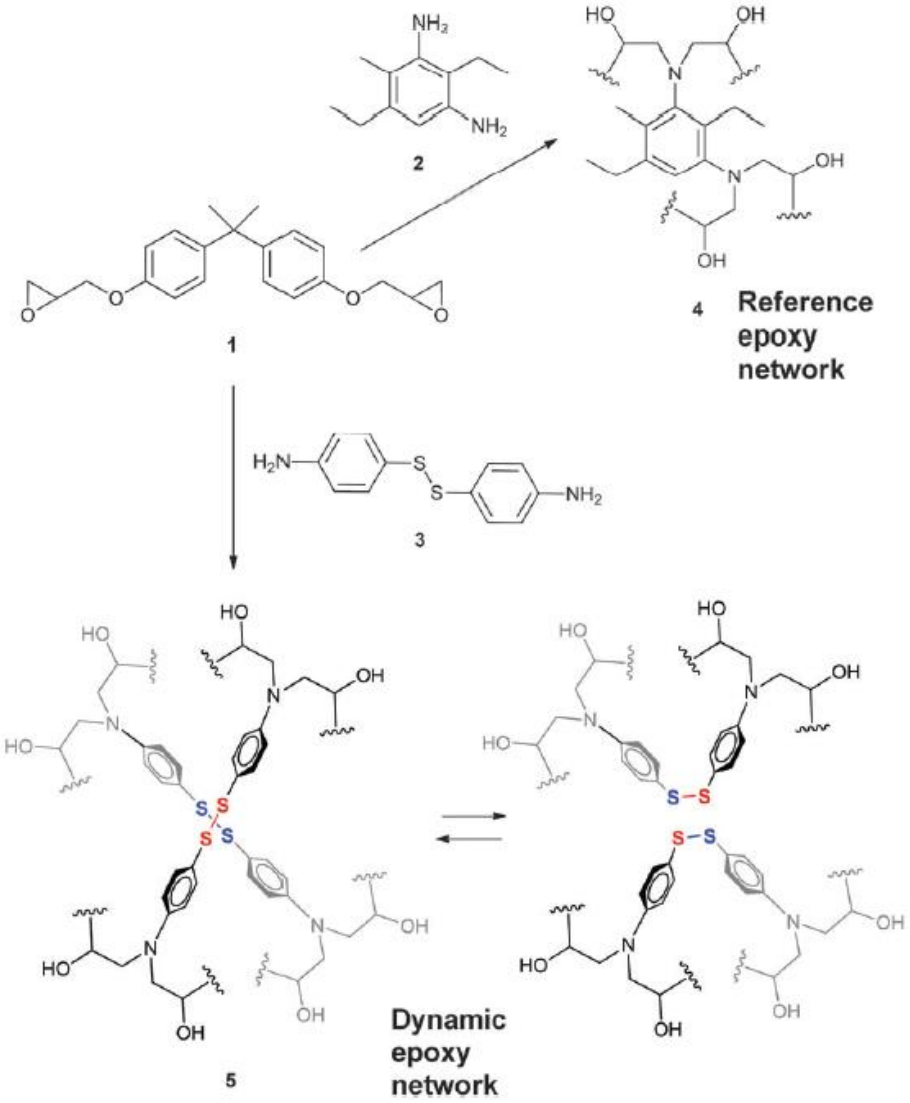

Figure 4 Synthesis and chemical structure of reference (thermoset) and dynamic (vitrimer) epoxy networks [6]

Vitrimers are typically synthesized by having the reaction of an epoxy resin with a specific hardener (usually contains amine, anhydride or carboxylic acid functions) that introduces dynamic covalent bonds into the network. In Figure 2 as an example, the synthesis begins with an epoxy resin which can be cured using different diamine hardeners depending on the desired network properties. To create the reference (thermoset) epoxy network in Figure 2, a traditional amine hardener was used meanwhile the vitrimer is formed with a disulfide-based hardener which leads to a dynamic crosslinked structure in which disulfide (S-S) bonds are the part of the network, and these S-S bonds are responsible for the bond exchange reactions that enable the vitrimer's dynamic behavior.

Figure 5 Reshaping of a vitrimer in few seconds with dynamic bond exchange (heat increasing) [7]

As mentioned, the covalent adaptable networks (CANs) in vitrimers enable bond rearrangement when triggered by an external stimulus such as heat [5]. When heat is applied, the associative exchange of disulfide bonds allows the crosslinked network to rearrange its bond configuration without breaking down the structure which shows the vitrimers thermally activated reprocessability. This process requires the vitrimer to be in its viscous state to enable bond exchange, which is why heat is used as the external stimulus rather than alternatives like light.

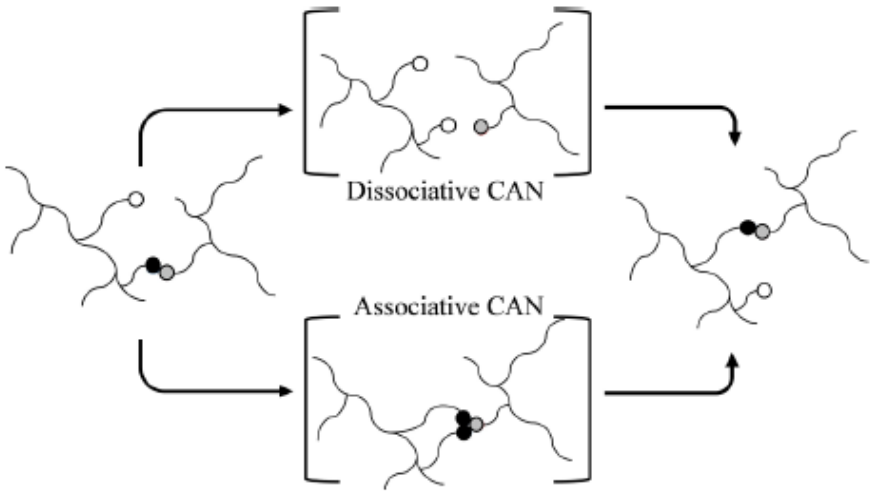

Figure 6 Dissociative and associative covalent adaptable network bond exchange reactions [8]

Covalent adaptable networks have two different bond exchange mechanisms (dissociative and associative). In dissociative covalent adaptable networks (CANs), a bond is first broken, and then a new bond is formed with a different site within the polymer network. In contrast, associative CANs initiate bond formation with a new partner before the original bond is broken, maintaining the network connectivity throughout the exchange process [9]. Since these mechanisms are correlated with the network connectivity and viscosity during thermoforming, they also affect the reprocessability of the polymers. In the case of vitrimers, the bond exchange follows an associative mechanism, which allows the material to retain its crosslinked structure even during dynamic rearrangement, providing a balance between stability and reprocessability that is critical for applications involving reshaping or healing under heat.

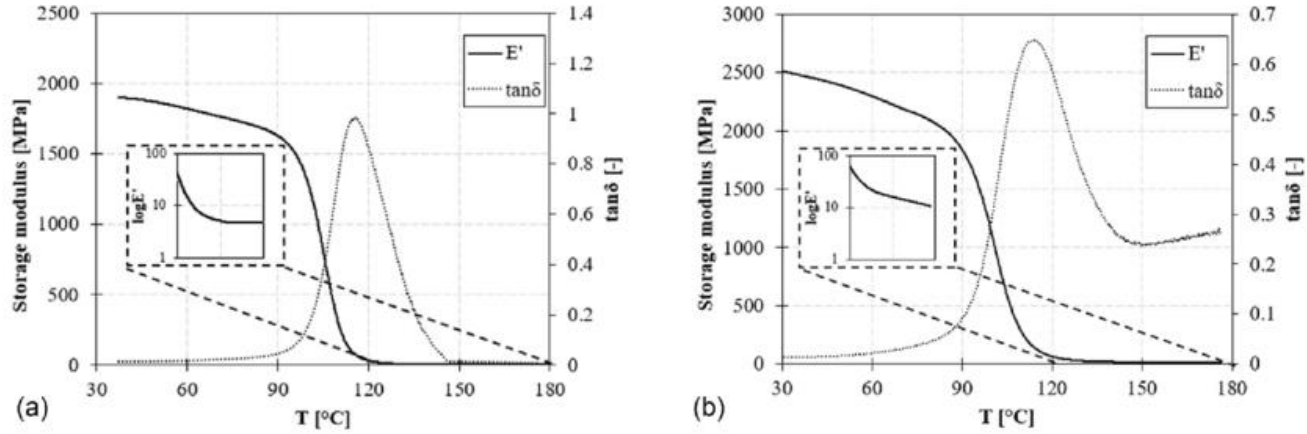

Figure 7 DMA curves of the (a) Standard Epoxy system and (b) Vitrimer [10]

Figure 5 DMA curves of the (a) Standard Epoxy system and (b) Vitrimer [10]

As observed in Figure 5, adapted from the study by Perna et al., the vitrimer sample (b) exhibits a secondary peak in the tan δ curve beyond 150 °C, in contrast to the epoxy system (a), which shows a continuous decrease in modulus and no such peak due to thermal degradation. This secondary peak in the vitrimer is attributed to the associative bond exchange mechanism, specifically the dynamic rearrangement of disulfide (S–S) bonds within the network structure [11]. While the peak is not highly pronounced in this specific dataset, it indicates the onset of topological rearrangement as the vitrimer transitions into its viscous, reprocessable state. A DMA characterization will be conducted in this study for both epoxy (up to 280 °C) and vitrimer samples (up to 250 °C), aiming to clearly capture this secondary transition in the vitrimer sample. It is expected that this extended analysis will also make the correlation with the storage modulus more observable, where a slight increase in modulus may be observed during the viscous flow regime and bond exchange peak, reflecting the vitrimer's ability to rearrange.

Table 3 Properties of vitrimer matrix

Matrix	Density (g/cm^3)	Failure Strain (%)	Tensile Strength (MPa)	Young's Modulus (GPa)	Glass Transition Temp. (°C)	Bond Exchange Temp. (°C)
RTM6-2	1.142-1.148	5.37-6.53	87.5-92.5	3.05-3.17	-16.7	222.5
RTM6-V	1.266-1.268	2.07-2.61	55.6-65.2	3.25-3.31	-10.6	232.5
HTG240-V-1/1	0.86-0.91	2.68-2.76	49-51	2.37-2.53	-7	>210
HTG240-V-1/1.2	0.84-0.89	1.36-1.44	30-44	2.36-2.40	-8	>210

When comparing vitrimer matrices to conventional thermoset and thermoplastic matrices, it is observable that vitrimers can exhibit properties similar to both types of polymeric matrices. For instance, HTG240-V-1/1 and HTG240-V-1/1.2 show relatively low densities (0.84–0.91 g/cm^3) compared to epoxy (1.1–1.14 g/cm^3) and polyester (1.2–1.5 g/cm^3), which can be advantageous for lightweight applications. Their tensile strengths (30–51 MPa) are lower than high-performance epoxies (35–100 MPa) but fall within or above the range of some thermoplastics. Similarly, their Young's moduli (2.36–2.53 GPa) are slightly lower than epoxy but higher than many thermoplastics. Glass transition temperatures for these vitrimers (around –7 to –8 °C) are significantly lower than conventional thermosets, reflecting their dynamic covalent network's ability to rearrange under certain conditions. To note, vitrimer properties can vary depending on the properties of their dynamic bonds. z

The reprocessability of vitrimers represents a significant advancement for both the industry and the environment, addressing one of the major limitations of traditional thermoset composites: their irreversibility and inability to be recycled. Conventional recycling methods for thermoset composites, such as pyrolysis or solvolysis, often degrade the matrix and fibers, limiting reuse and increasing waste. In contrast, vitrimers, through their dynamic covalent networks, enable reshaping, repairing, and full recycling without sacrificing huge amount of material [12].

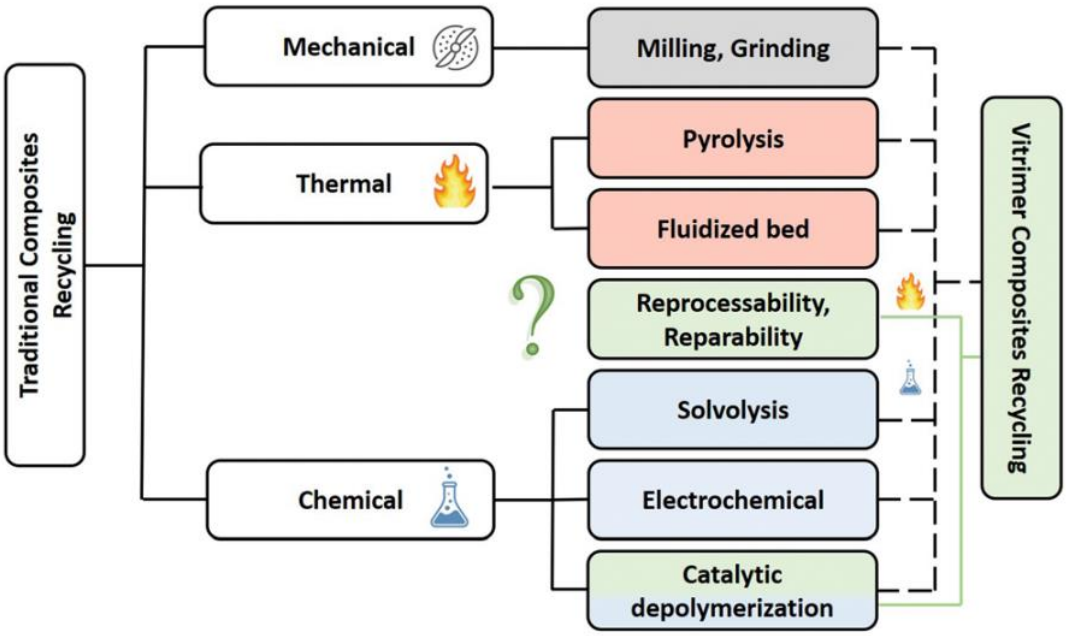

Figure 8 Classification of the major recycling methods of traditional composites with possible alternatives offered by vitrimer composites [13]

This innovation of recyclable composite matrix aligns perfectly with the growing industrial demand for sustainable materials, especially in sectors such as aerospace, automotive, and wind energy, where lightweight, strong, and durable composites are needed. Current research and industrial initiatives have begun integrating vitrimer matrices into carbon fiber reinforced polymers (CFRPs). In the current stage of development, vitrimer technologies are mostly being explored by start-ups such as Mallinda and ATSP Innovations, as well as through funded research projects like AIRPOXY, ECOXY and VITRIMAT which are funded by the European Union [13].

2.2.Manufacturing of Vitrimer Matrix Composites

The selection of a manufacturing process for composite part production is influenced by multiple factors, including (i) the nature of the constituent materials (such as fibers and matrix) and their forms (e.g., rovings, chopped fibers, unidirectional reinforcements, textiles), (ii) the required mechanical performance, (iii) the desired production throughput (ranging from single parts per day to mass production volumes), and (iv) cost considerations [14].

Manufacturing methods for vitrimers are still under investigation and active research, considering the parameters described above as well as current literature knowledge; therefore,

this section will discuss processes such as resin transfer moulding, hand lay-up with vacuum bagging, and filament winding.

2.2.1. Resin Transfer Moulding (RTM)

The resin transfer moulding (RTM) process involves placing the preform, consisting of a porous fibrous reinforcement shaped to match the final part, inside the mold. Once the mold containing the preform and residual air is closed, resin is injected into the cavity until the reinforcement is completely impregnated. Following the resin curing stage, the mold is opened, and the composite part is demolded. Additional finishing steps or post-curing may still be required. The RTM mold design must incorporate at least one inlet port for resin injection and one outlet to allow air to escape during the injection process [15]. The methodology is well-suited for mass production and large-scale industrial applications, with numerous studies exploring the influence of material properties and processing parameters on its performance. Recently, RTM has also been investigated as a promising fabrication method for vitrimer matrix composites, due to its ability to produce high-quality, reproducible parts.

Several recent studies have demonstrated the feasibility of manufacturing vitrimer matrix composites using the resin transfer moulding (RTM) process. For instance, Schenk et al. (2023) developed a high-performance epoxy vitrimer based on an aeronautics-grade resin, achieving the highest reported vitrimer glass transition temperature (233 °C) and establishing a comprehensive time–temperature–transformation (TTT) diagram to guide RTM processing parameters [7]. In another study, Schenk et al. (2024) compared the performance of carbon-fiber-reinforced laminates using both conventional RTM6 epoxy and a vitrimer system with a disulfide-based hardener, showing promising mechanical properties, acceptable water absorption, and potential for limited repair of impact-induced damage [16]. Additionally, Schenk et al. (2024) investigated a new epoxy vitrimer formulation with disulfide exchange chemistry tailored for RTM, again constructing a TTT diagram to optimize processing and demonstrating reprocessability and mechanical characteristics comparable to reference epoxies [17]. Martinez and Nutt (2024) further explored flax-reinforced vitrimer epoxy composites manufactured by RTM, showing that these laminates offered equivalent flexural strength and tensile modulus to conventional aerospace epoxy composites, albeit with a slight reduction in tensile strength [18]. Collectively, these studies highlight RTM as a promising and increasingly validated technique for the scalable production of vitrimer-based composite structures.

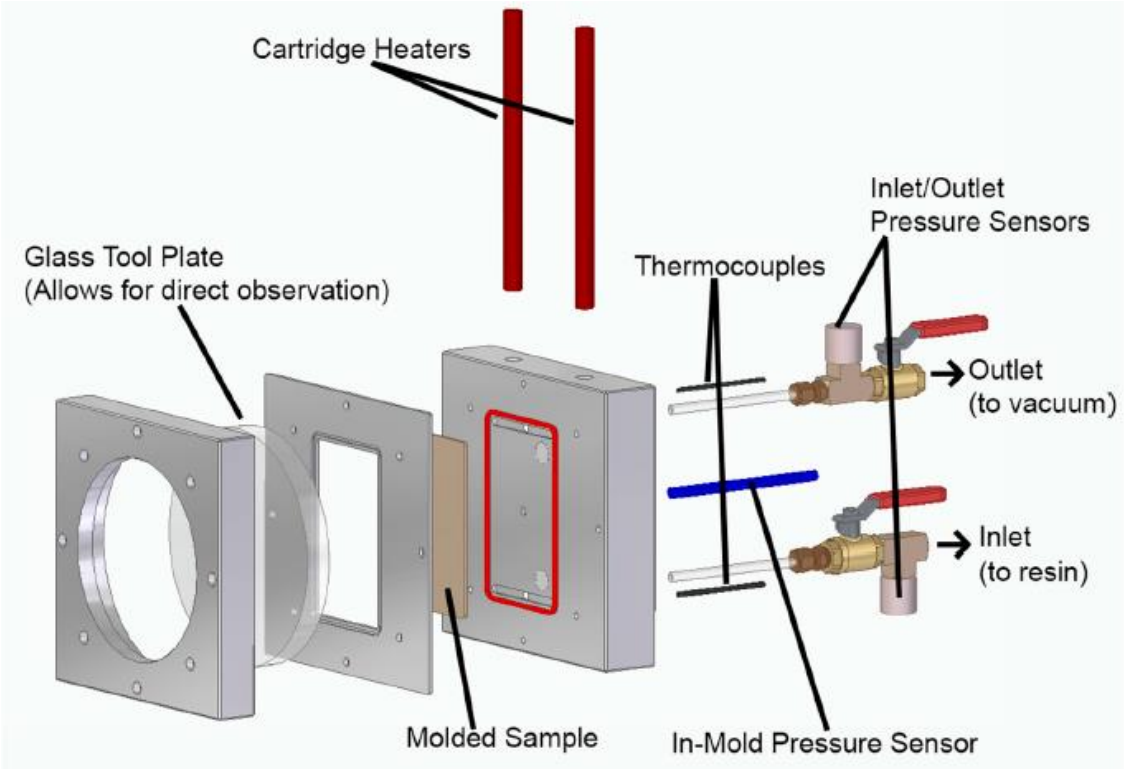

Figure 9 RTM test cell to produce laminates in study of Martinez and Nutt [18]

Figure 7 shows the RTM setup developed by Martinez and Nutt for vitrimer matrix composite manufacturing. The vitrimer resin was mixed and vacuum-degassed for 5 minutes, then heated to 55 °C in a pressure pot. The mold was preheated to the same temperature, and resin infusion was carried out under 350 kPa pressure. After full impregnation, the outlet was sealed, and the mold was heated to 150 °C for 60 minutes, followed by a 60-minute post-cure at 180 °C.

2.2.2. Filament Winding

Filament winding is a composite manufacturing technique used primarily to produce hollow, cylindrical, or prismatic components such as pipes, tanks, and pressure vessels. In this process, continuous fiber tows are guided and wound around a rotating mandrel in a specific geometric pattern using a controlled delivery system. The winding angle—defined by the fiber's orientation relative to the mandrel's axis—is a key parameter that influences the final part's strength and stiffness alongside winding tension and time. The process can be executed in two variations: wet winding, where fibers are impregnated with resin just before application, and dry winding, which uses pre-impregnated materials. After winding the desired number of layers, the part is typically cured in an oven while on the mandrel. Filament winding allows for precise control of fiber orientation and resin content, making it highly efficient and suitable for producing structurally optimized parts [19]. Filament winding is considered an appropriate

method for vitrimer matrix composite manufacturing due to its ability to produce high-quality, fiber-reinforced structures with controlled architecture of specific kinds, while having the potential of accommodating the thermal conditions needed for vitrimer curing and a potential reshaping.

Recent research has begun to explore the integration of vitrimer matrices into filament winding processes, particularly wet filament winding, to enable recyclable and reprocessable composite structures. Alms et al. (2025) demonstrated the feasibility of producing carbon fiber-reinforced vitrimer composites at an industrial scale using a wet filament winding setup, focusing on type-4 pressure vessel demonstrators. Their study compared two vitrimer formulations to a conventional epoxy thermoset, revealing enhanced interlaminar shear strength at both room temperature and elevated temperatures. However, achieving a pore-free composite remained a challenge, indicating the need for further optimization of processing parameters for vitrimers [20]. Complementing this work, Lorenz et al. (2024) conducted a detailed material characterization and modeling of an epoxy vitrimer based on disulfide exchange for wet filament winding applications. By comparing vitrimeric and traditional epoxy resins, the study highlighted the necessity of adjusting resin bath temperatures to ensure successful processing [21]. Despite these adjustments, the mechanical properties, such as elastic modulus and compression behavior, were found to be comparable between the two systems. These findings suggest that with proper adaptation, existing filament winding setups can be effectively utilized for vitrimer matrix composites, advancing their application in recyclable and high-performance composite manufacturing.

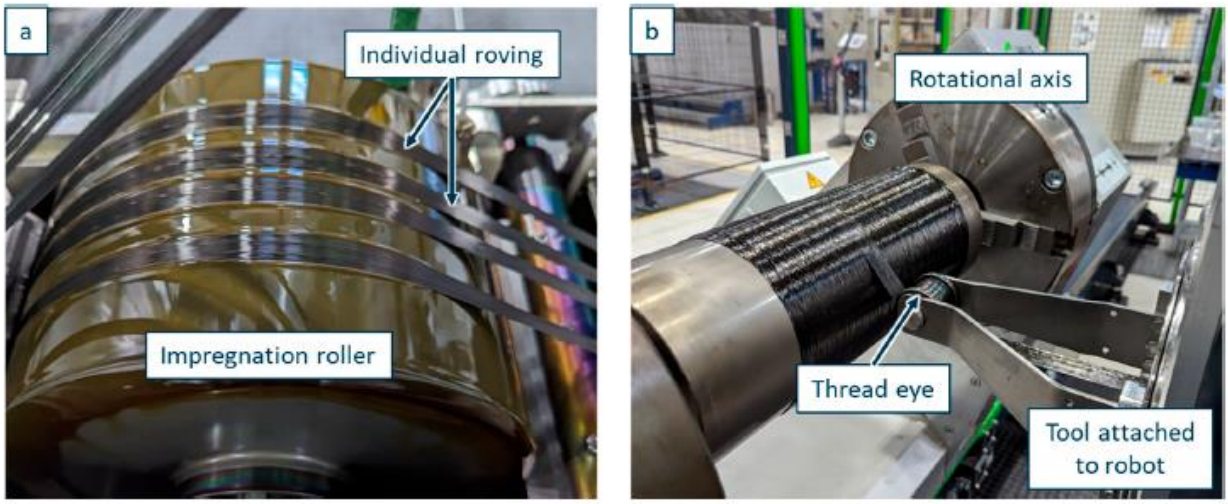

Figure 10 Production of CFRP with vitrimeric matrix material. (a) Roller for filament [20]

The filament winding process described is based on the work by Alms et al., where a robotic setup was used to manufacture carbon fiber reinforced vitrimer matrix composite pipes. In this study, the vitrimer resin and curing agents were preheated to achieve suitable viscosity for effective fiber impregnation. The impregnated fibers were wound onto a mandrel to form multiple hoop layers, using consistent processing parameters. Slight adjustments in resin bath temperature were made depending on the vitrimer formulation to ensure optimal resin flow. Figure 8 illustrates the setup, showing the impregnation roller and the fiber deposition process on the rotating mandrel.

2.2.3. Hand Layup, Vacuum Bagging & Compression Moulding

Hand lay-up combined with vacuum bagging is a widely used composite manufacturing method, especially suited for small-scale production, prototyping, and academic research due to its low equipment cost and process simplicity. In hand lay-up, dry or prepreg reinforcement are manually placed into an open mold and if the reinforcement is dry it is impregnated with resin using brushes or rollers. This technique allows for significant control over fiber orientation and stacking, although it requires skilled handling to ensure uniformity and proper wet-out of the fibers, especially when dealing with thick fabrics or aiming for high fiber volume fractions [22].

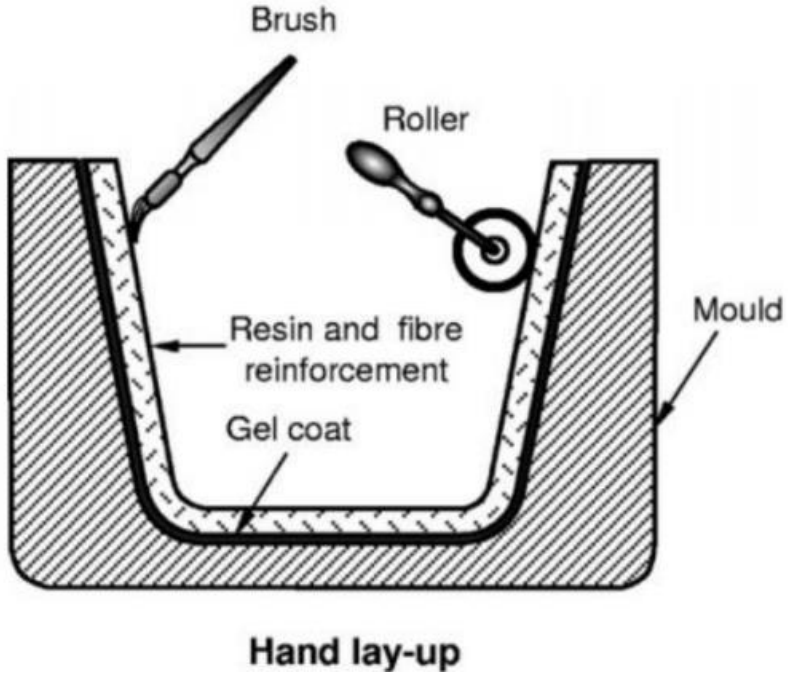

Figure 11 Typical hand-layup process with dry fibers [23]

Vacuum bagging is a technique used before curing to enhance the quality of composite laminates during manufacturing. After the layup process, a flexible vacuum bag is sealed over the laminate over a releasing agent, and air is evacuated using a vacuum pump. Vacuum bagging is especially common in research and small-scale production due to its low equipment cost and effectiveness in improving laminate quality by reducing the amount of porosity and air bubbles inside and between the plies. Figure 12 presents a schematic representation of a typical vacuum bagging system used after hand layup composite manufacturing. In this process, the laminate is placed on a mold and covered with several layers, including a peel ply, breather, and bagging film, which are sealed around the edges with sealant tape. A vacuum pump, connected through tubing and a valve system, applies negative pressure to compact the laminate, remove trapped air, and assist resin distribution. This setup provides improved consolidation of the composite structure and minimizes void formation during curing.

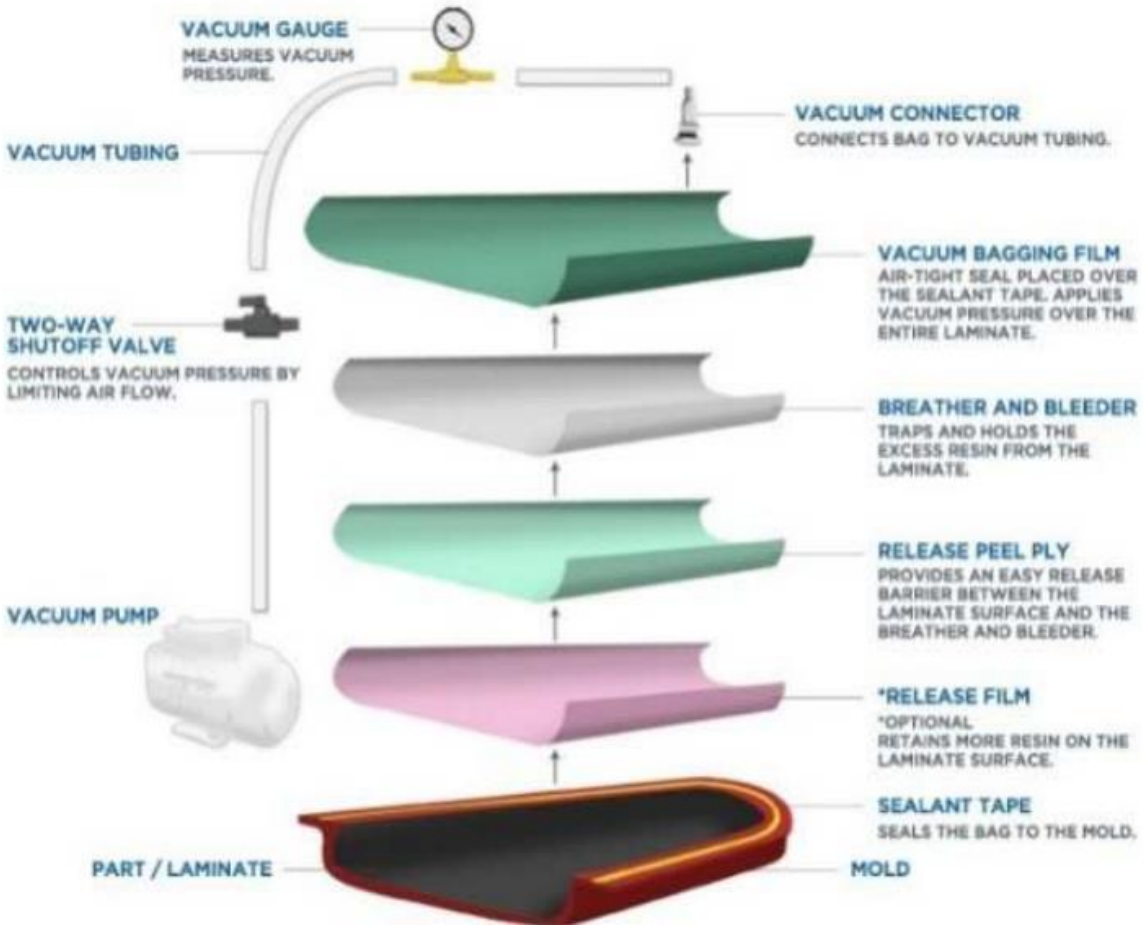

Figure 12 Classical vacuum bagging setup [23]

Also in this study, all composite samples used for various characterization tests were manufactured using hand lay-up combined with vacuum bagging technique. While further details on the fabrication of specific samples will be provided in subsequent sections, it is

important to note that vitrimer-based samples were prepared using prepreg materials to ensure consistent resin content and fiber distribution. In contrast, reference and verification samples with conventional epoxy matrices were produced through wet lay-up, involving manual impregnation of dry fabrics with liquid resin. This dual approach allowed for appropriate comparison between vitrimer and traditional epoxy systems under consistent processing conditions. After the layup, an optimum vacuum bagging setup was applied after several attemps with different elements, or with the same elements positioned differently.

THIS PAGE WAS INTENTIONALLY LEFT BLANK

3. EXPERIMENTAL ANALYSIS

3.1. Thermal Characterization of Vitrimer Matrix

Before initiating composite manufacturing and additional testing on vitrimer matrix composites, a preliminary thermal characterization of the vitrimer matrix itself was conducted. The aim of this step was to understand the fundamental thermal behaviour of the matrix material, particularly in relation to the covalent adaptable network (CAN) and its bond exchange mechanisms that become active beyond the glass transition temperature (Tg). For this, Dynamic Mechanical Analysis (DMA), Differential Scanning Calorimetry (DSC) and Thermomechanical (TMA) tests were performed on the vitrimer resin.

3.1.1. Dynamic Mechanical Analysis

Dynamic Mechanical Analysis (DMA) is a thermal-analytical technique that measures the mechanical response of polymeric materials when subjected to an oscillating force. By tracking the relationship between the applied stress and the resulting strain over a range of temperatures and frequencies, DMA allows the evaluation of key viscoelastic properties such as storage modulus (elastic behavior), loss modulus (viscous behavior), and damping (tan δ) which is the ratio between two modulus values. These properties offer insights into how a polymer stores and dissipates energy. DMA is particularly effective at identifying material transitions, such as glass transition (Tg), melting points for thermoplastics, and decomposition onsets in both thermoplastics and thermosets by the peaks in the curve. Compared to other thermal techniques like DSC or TGA, DMA is more sensitive to molecular motion and structural relaxation, making it highly suitable for evaluating thin films, coatings, and highly crosslinked thermosets [24].

The primary purpose of DMA in polymer characterization is to characterize the critical thermal and mechanical transition points that define material properties. For thermoplastics, DMA can detect the glass transition temperature (Tg), melting point (Tm), and changes in modulus that reflect the shift from glassy to rubbery to viscous behavior. For thermosets, the technique is used to monitor Tg and the onset of decomposition, which often coincides with a drop in modulus due to structural breakdown or a peak in tan δ curve. DMA is especially advantageous in detecting subtle transitions and identifying the influence of additives, fillers, or crosslinking

agents on polymer properties that might not be captured through other thermal characterization techniques like DSC or TGA [25].

In the case of this study, Dynamic Mechanical Analysis (DMA) was performed on both reference epoxy and the vitrimer samples to evaluate and compare their thermal and viscoelastic behavior. The reference sample served to verify the reliability of the experimental setup and to provide data for comparison, while the vitrimer matrix was characterized to observe its distinct thermal transitions and dynamic bond exchange characteristics. The DMA experiments were conducted using the testing equipment shown in Figure 12, the Metravib DMA+100 (maximum of 100N static force) system. The system features a rigid mechanical frame, optimized electronics, and displacement signal measurement technologies which measures viscoelastic and thermal properties of polymeric and composite materials. The specimen is placed between the clamps or holders that are selected according to the tension test mode. The system applies a static force with an osciallatory frequency to the sample while simultaneously measuring the resulting displacement, than the same with the displacement.

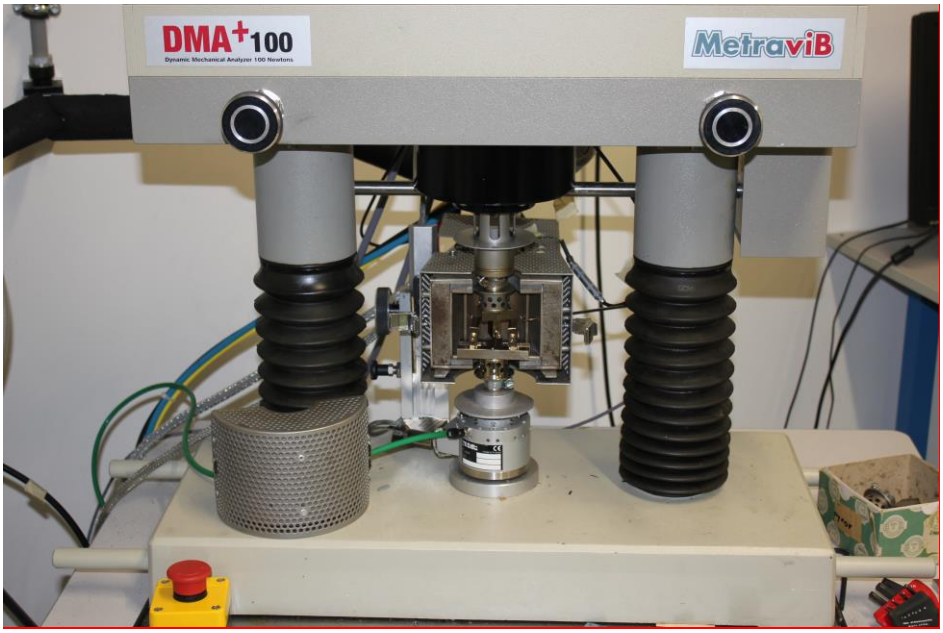

Figure 13 Sample placement spot of the DMA machine (Metravib DMA+100) used

The DMA testing on vitrimer matrix was conducted in two phases. In the first phase, a constant room temperature was maintained while the samples were tested at three different frequencies (1, 10 and 100 Hz) with a constant static force of 2 N. This step aimed to determine the linearity between storage/loss modulus and dynamic displacement, allowing the identification of a reasonable dynamic displacement value that provides accurate results within the linear viscoelastic region. Based on the most linear segments observed in the modulus-displacement curves, an optimal displacement value was selected for further thermal analysis.

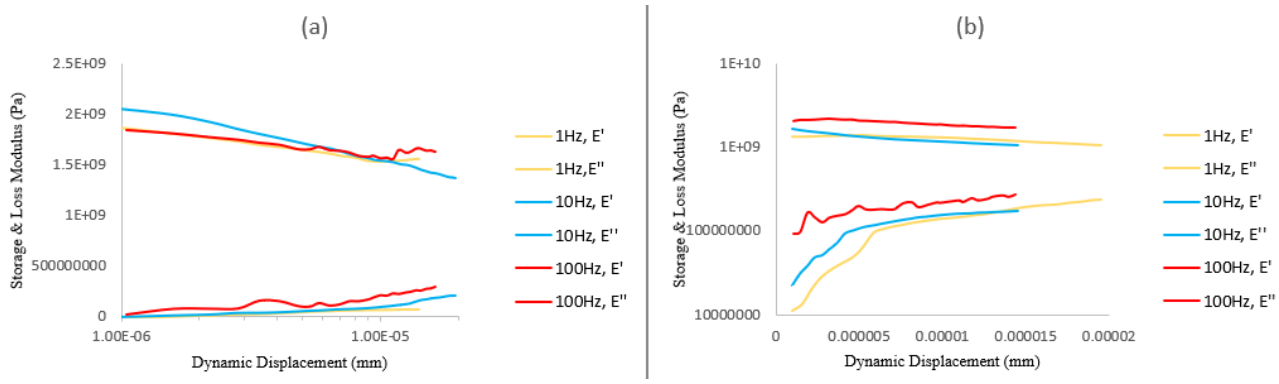

Figure 14 Evolution of Storage (E') and Loss (E") Modulus depending on the applied dynamic displacement for reference epoxy network (a) and vitrimer (b) samples applies on different frequencies

Based on the results shown in Figure 10, the dynamic displacement–modulus behavior was evaluated across three different frequencies for both the reference epoxy and vitrimer samples. Among these, the 1 Hz frequency curves exhibited the most consistent and linear behavior, particularly in the loss modulus (E″) responses. This linearity is critical for knowing that the material is tested within the linear viscoelastic region, which is needed for accurate thermal analysis. While it might be possible to state that lower frequencies provide more stable and smooth modulus-dynamic displacement responses, further reduction of frequency to 0.5 Hz was not possible in this case due to insufficient displacement output. From the 1 Hz modulus curves, the region around a dynamic displacement of around 5 µm was determined as the most linear segment. This displacement value was therefore applied as the input parameter for the second phase of DMA testing.

In the second phase, this selected dynamic displacement was applied along with the same static force at varying frequencies while the temperature was gradually increased from room temperature to 270°C for epoxy reference and to 250°C for vitrimer samples. This thermal sweep was conducted to monitor the curves of storage modulus, loss modulus, and tan δ as a function of temperature. The main goal was to identify characteristic thermal transitions, particularly the glass transition temperature (Tg), and to detect the secondary tan δ peak in vitrimer systems related to the chemical bond exchange, which is associated with dynamic disulfide bond exchange, as referenced earlier in Figure 5. As a secondary goal, the effect of increasing frequency was observed on the curves and peaks.

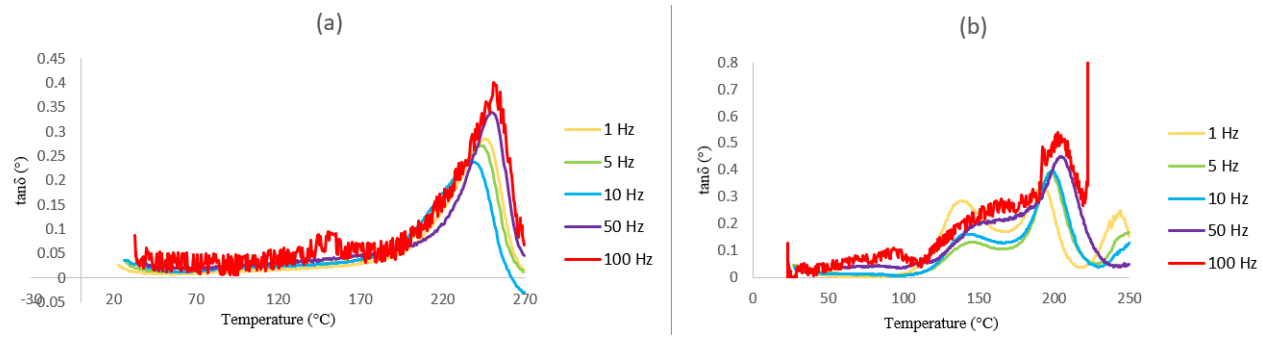

Figure 15 Tan δ - Temperature curves of reference (a) and vitrimer (b) samples

As can be seen in Figure 8, the temperature-dependent tan δ curves for the vitrimer and reference thermoset epoxy samples display different thermal behaviors. In the reference sample, a single, sharp tan δ peak is observed around 240–250 °C, which is associated with the glass transition temperature (Tg), followed by a rapid decline indicating the start of thermal degradation around 250 °C when the curve is linear. In contrast, the vitrimer sample exhibits a wider primary glass transition region and the initiation of a secondary peak near 180-200 °C, which is related to the dynamic disulfide bond exchange characteristic of vitrimer networks. This secondary transition reflects the onset of bonding rearrangement within the vitrimer structure under thermal activation, seperating it from the irreversible degradation behavior of traditional thermosets. The influence of frequency is not clearly systematic across the curves; the positions of the peaks do not consistently shift with increasing frequency, suggesting that thermal instability or sample-specific (humidity, errors etc.) factors may have an affect on the response expect the secondary peak regions for vitrimers, which a frequency effect can be observed on the height of the secondary peak related to the dynamic bond exchange mechanism. Additionally, 100 Hz curves exhibit significant distortion, and the vitrimer sample showed visible thermal damage beyond approximately 225 °C, which may have limited data quality at higher frequencies.

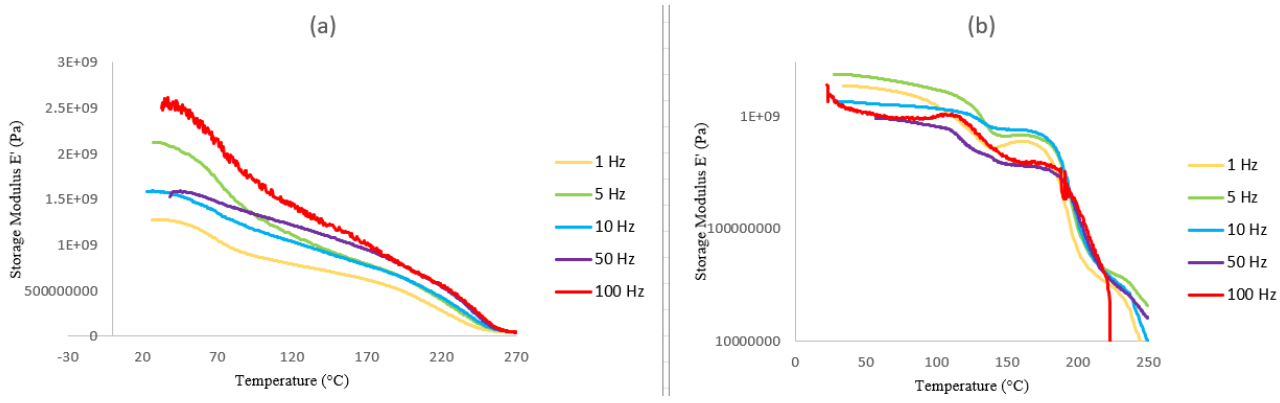

Figure 16 Storage modulus - temperature curves of reference (a) and vitrimer (b) samples

As seen in Figure 12, the temperature-dependent storage modulus (E′) curves for both the reference epoxy and vitrimer samples demonstrate the typical modulus decrease with increasing temperature, corresponding to the softening and molecular mobility in the network structures. For the reference thermoset epoxy, a gradual decline in E′ is observed across all frequencies, with the modulus decreasing significantly after ~220 °C, marking the approach to thermal degradation. The overall stiffness of the material decreases as it transitions through the glass transition region, and no modulus recovery is observed beyond this point, consistent with the irreversible network structure of conventional thermosets. On the other hand, the vitrimer sample shows a plateau in E′ up to approximately 180–200 °C which is aligned with the tan δ curves, after which a sharp modulus drop occurs. The distortions in the 100 Hz curve, especially beyond 200 °C, reflect thermal instability and mechanical damage, likely due to material degradation or slipping during testing. These findings support the thermomechanical difference between the two materials: the reference epoxy follows a typical thermoset modulus decline, while the vitrimer exhibits behavior characteristic of dynamic network rearrangement before degradation.

3.1.2. Differential Scanning Calorimetry

Differential Scanning Calorimetry (DSC) is a widely used thermal analysis technique that helps determine the thermal transitions of polymers and composites by measuring the heat flow associated with temperature changes. In a typical DSC setup, a sample and an empty reference pan are heated at the same rate, and the instrument tracks the difference in heat required to maintain equal temperature increases in both pans. From this, information such as the glass transition temperature (Tg), melting temperature (Tm) and crystallization temperatures (Tc), for thermoplastics, enthalpy changes, and specific heat capacity (Cp) can be retrieved. DSC is particularly effective in identifying phase transitions, such as glass transition, melting and crystallization, which involve endothermic or exothermic heat flows. It is sensitive to transitions that involve changes in heat capacity, such as the glass transition, even if there is no latent heat involved. Compared to Dynamic Mechanical Analysis (DMA), which measures mechanical properties like storage modulus, loss modulus, and damping factor as a function of temperature, DSC is only capable of measuring thermal energy changes.

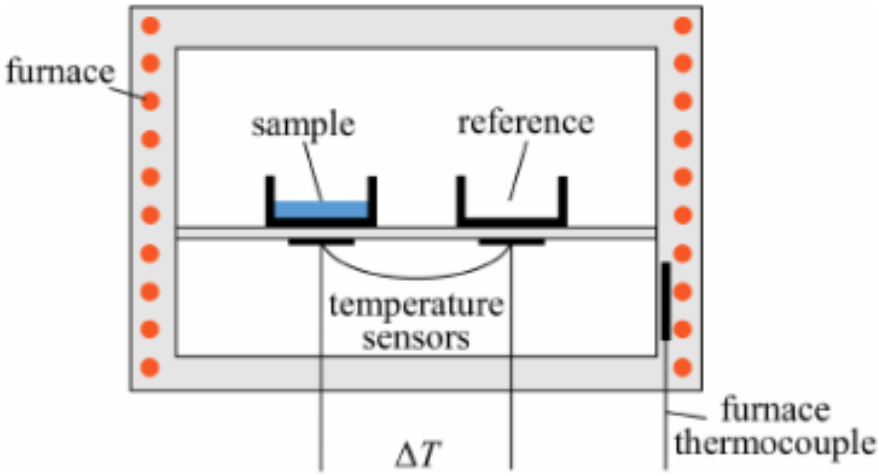

Figure 17 Setup of a conventional heat flux differential scanning calorimeter

For DSC analysis of the study, TA Instruments DSC Discovery Series was used which can be observed in Figure 17. The instrument is designed to measure heat flow associated with transitions in materials, such as glass transition, melting and an expected dynamic bond exchange for vitrimers. For the DSC analysis, the sample is placed into a small aluminum or hermetically sealed pan with a little hole, which is then loaded into the furnace near the reference pan so that the instrument can measure the difference in heat flow between the two as the programmed temperature cycle is applied.

Figure 18 Sample placement spot of the DSC machine (TA DSC Discovery Series) used

In this study, DSC was employed to investigate the initial peaks observed in the DMA analysis of vitrimer samples, which were initially thought to be caused by residual humidity. Since DSC does not typically detect transitions associated with moisture content, it was chosen primarily as a verification method to confirm or rule out this hypothesis. However, as seen in the DSC graph on Figure 14, a peak appeared at the same temperature range as the one observed in the DMA analysis. This led to the rejection of the theory of the first peak being related to humidity or moisture inside the vitrimer material. Instead, the presence of this peak was interpreted as an indication of incomplete curing in the vitrimer network, suggesting that additional curing reactions or network rearrangements may still be taking place at elevated temperatures.

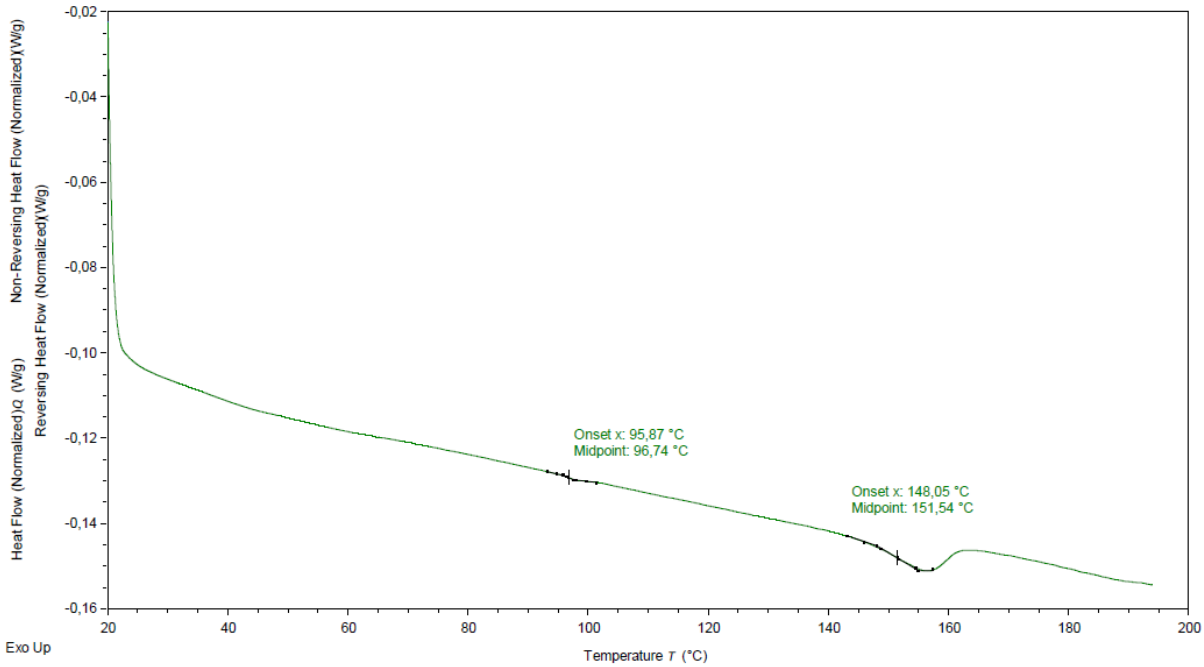

Figure 19 Differential scanning calormitery graph of heat flow versus temperature for vitrimer matrix

The DSC graph on Figure 14 of the vitrimer matrix shows two distinct transitions: the first peak appears around 95 °C (onset at 95.87 °C), and a second thermal event indicating the glass transition occurs near 151 °C (onset at 148.05 °C). This initial peak matches the first transition observed in the DMA analysis. Since DSC is not capable of detecting water loss or humidity-related transitions, this result confirms that the low-temperature DMA peak is not due to moisture content or humidity in the sample. Instead, the presence of a thermal event around 95 °C, together with a significantly lower-than-expected glass transition temperature (Tg), The observed thermal activity is likely due to post-curing or residual curing reactions occurring during the DSC scan.

3.1.3. *Thermomechanical Analysis*

As the final method used to characterize the vitrimer matrix, Thermomechanical Analysis (TMA) was employed to determine the coefficient of thermal expansion (CTE), to be used in analysis of stress relaxation behavior of vitrimer matrix composite. TMA is a fast and effective technique for measuring dimensional changes in a material such as expansion, contraction, or deformation under controlled temperature, time, and load conditions. In expansion mode which is used for this study, a small constant force is applied through a probe resting on the sample while the temperature is increased, allowing the detection of linear expansion, glass transitions, and softening behavior.

Figure 20 TMA equipment used (NETZCH Hyperion TMA 402 F3)

The TMA tests on vitrimer matrix were conducted using the NETZCH Hyperion TMA 402 F3 instrument, which is photographed in Figure 19. The equipment is designed to measure dimensional changes in solids, especially polymers as a function of temperature and/or time under a defined mechanical load. It is capable of determining the linear thermal expansion, softening points or glass transition temperatures of polymeric materials. The working principle of the TMA involves placing the specimen in a furnace chamber, where it is subjected to controlled heating or cooling while a push rod applies a defined force. The dimensional changes of the sample are detected through a displacement transducer, which converts the mechanical movement into a digital signal. This setup enables the instrument to capture even very small deformations with high accuracy.

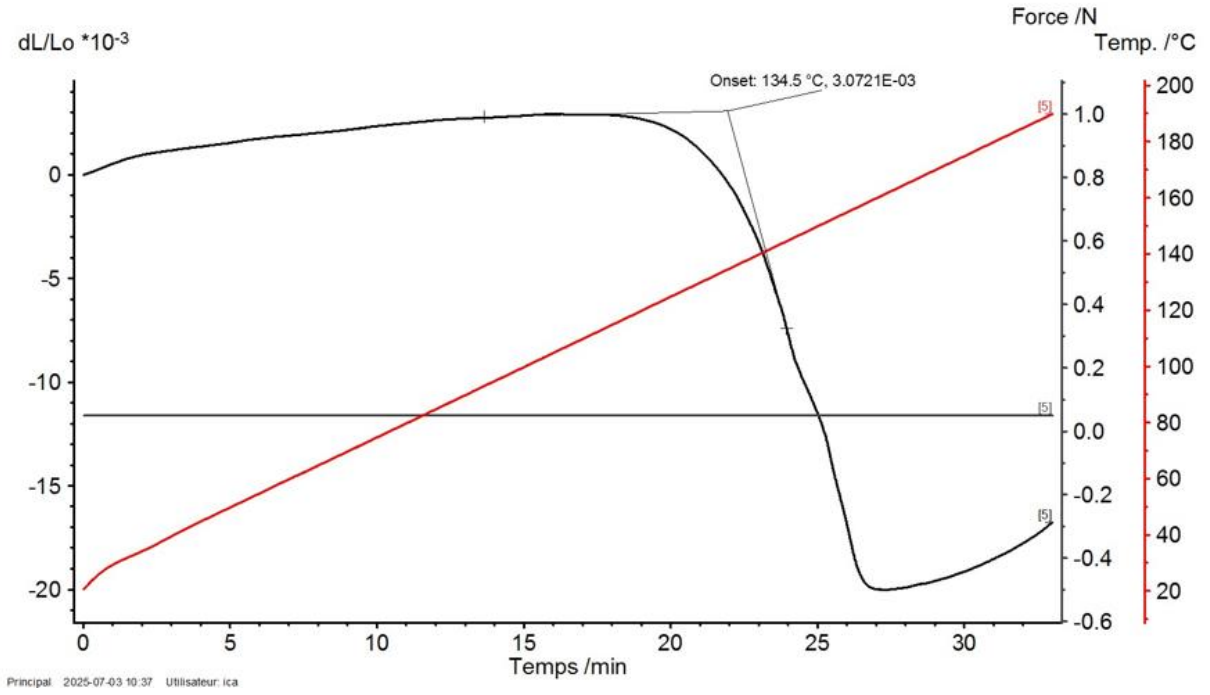

Figure 21 Graph of time-temperature-expansion obtained from TMA experiment

The vitrimer sample was subjected to a controlled heating and cooling cycle: it was heated from −60 °C to 190 °C at a constant rate of 5 °C/min, and then cooled down to −20 °C under the same rate. Throughout the test, a small constant force of 0.0005 N was applied via the probe, and an inert helium atmosphere was maintained to provide thermal stability to the system. COMMENT ABOUT THE GRAPH?

3.2. Vitrimer Matrix Composite Sample Production

After characterizing the vitrimer matrix, composite samples reinforced with carbon fibers were fabricated using hand lay-up and vacuum bagging techniques, followed by a thermal curing process as previously described. Different sample geometries, ply orientations, and lay-up configurations were prepared to suit the requirements of different characterization methods. It might be noted that all vitrimer composite samples were produced using prepreg unidirectional carbon fibre fabrics already impregnated with the vitrimer matrix.

The first set of composite samples was manufactured for impedancemetry studies. These consisted of $[0°]_8$ laminates with square geometries (100 mm × 100 mm). For a second round of impedancemetry tests, two additional samples were prepared with the same base geometry but included embedded electrodes placed between the last two plies on each side, resulting in a $[0°]_{10}$ configuration. These were cured in a custom setup with electrodes and connecting wires

integrated, which will be described in detail (curing cycle, heat flow etc.) in the impedancemetry section.

The second type of samples was designed for stress relaxation experiments. These were produced in multiple batches to induce internal stresses and generate curvature upon curing. The base configuration used a $[0/90]_2$ lay-up in a 20 mm × 200 mm mold. Again, vitrimer prepreg fabrics were used. For reference and validation purposes, additional epoxy-based samples were manufactured with the same orientation and geometry, but in this case, manual impregnation (wet lay-up) was used during fabrication. To enhance internal stress for comparison, additional samples with a [0/0/90/90] lay-up were also prepared, both using vitrimer and conventional epoxy matrices. Additionally, to exploit the difference in thermal expansion coefficients between aluminum and vitrimer matrix composites, two bimaterial samples were produced using the same 20 mm × 200 mm geometry. These consisted of two 90° prepreg plies laid directly on aluminum substrates and cured together, aiming to induce curvature and residual stresses upon cooling due to the mismatch in thermal behavior.

Figure 22 Two types of stress relaxation samples (a): $[0/90]_2$ (b): [0/0/90/90]

Figure 21 shows the two types of ply orientations that were prepared for stress relaxation testing. Laminate (a) corresponds to a $[0,90]_2$ layup, while laminate (b) corresponds to a [0/0/90/90] sequence. These schematic representations are included to clarify the laminate structures used in the stress relaxation experiments and to highlight the distinction between the two stacking sequences. Also, these two type of ply orientations had effect on stress relaxation behavior of laminates as will be discussed in detail in the stress relaxation section of this study.

Table 4 Samples produced with hand-layup & vacuum bagging for studies

Sample	Matrix Type	Ply Orientation	Geometry (mmxmm)	Imprengation Type
Impedancemetry	Vitrimer	$[0]_8$	100x100	Prepreg

Impedancemetry	Vitrimer	$[0]_{10}$	100x100	Prepreg
Stress Relaxation	Vitrimer	$[0/90]_2$	20x200	Prepreg
Stress Relaxation	Reference Epoxy	$[0/90]_2$	20x200	Impregnation
Stress Relaxation	Vitrimer	[0/0/90/90]	20x200	Prepreg
Stress Relaxation	Reference Epoxy	[0/0/90/90]	20x200	Impregnation
Stress Relaxation	Vitrimer	$[90]_2$	20x200	Bi-material

For all the samples, the same vacuum bagging principles were applied prior to curing, with slight modifications made over the progress of the study to optimize the process. Initially, the setup included a layer of breather textile placed between the releasing agent and the steel mold. However, after producing the first batch of stress relaxation samples, this lower breather layer was removed. The top breather layer alone was sufficient for the air evacuation which made the bottom layer unnecessary since the layer prevented the increase of stress created by the difference on thermal expansion coefficient between the mould and the composite. Also, polyamide film was originally used as the releasing agent during the first curing cycle. This material adhered too strongly to the vitrimer surface which caused a difficult demolding and risking damage to the sample. As a result, it was replaced with a more suitable releasing film in later manufacturing steps.

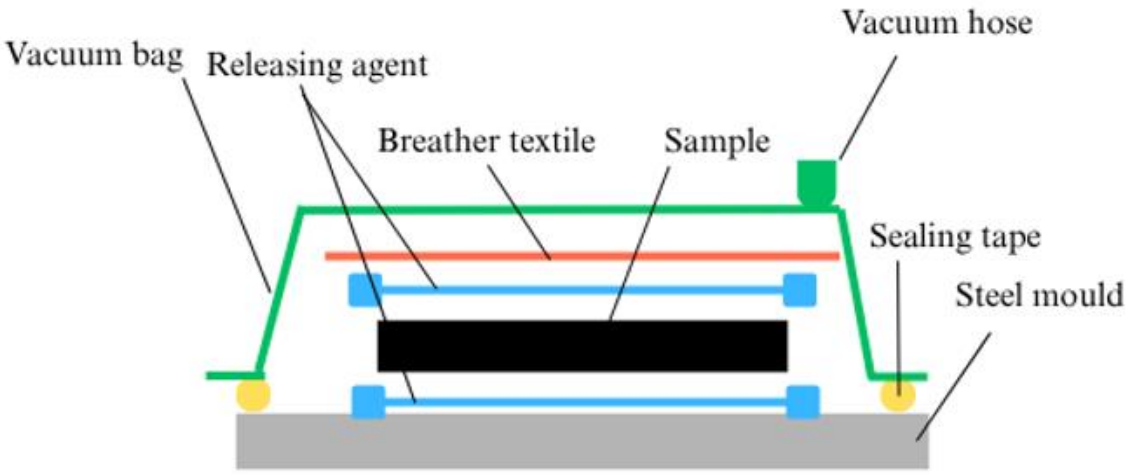

Figure 23 Final setup of vacuum bagging system

Figure 14 illustrates the final vacuum bagging setup used for vitrimer and reference epoxy matrix composite laminate sample production. The lay-up is carried out on a steel mold (not in direct contact, protected with polyamide or releasing agent), with a releasing agent applied around the laminate to prevent it from adhering to the mold surface during curing, allowing for easy demolding. On top of the sample, a breather textile is placed which provides uniform vacuum distribution and allows the removal of trapped air. Without the breather, localized pressure zones or air pockets could develop, compromising the laminate's quality. The entire system is then enclosed in a vacuum bag, which is sealed tightly to the mold surface using

sealing tape around the perimeter. A vacuum hose is connected to extract the air inside the bag using a pump. Two main motivations of this setup are to compact the laminate layers and reduce the void content by eliminating trapped air during hand layup. Once the vacuum is applied and the air is fully removed, the bagged systems with different samples are moved in a freezer to preserve the prepreg material's reactivity before it is cured, ensuring that no unwanted curing takes place at room temperature before the oven.

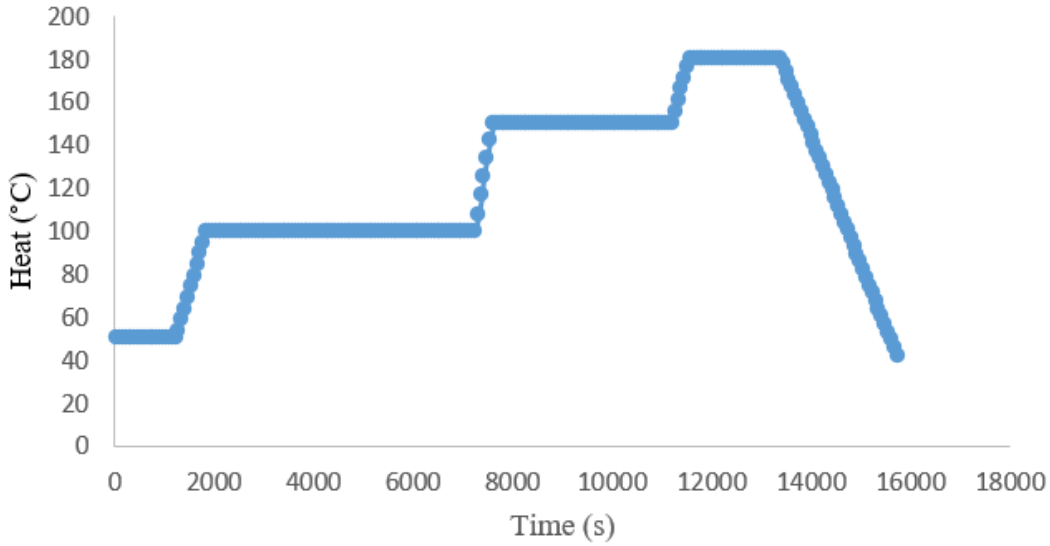

Figure 24 Curing cycle used for vitrimer matrix composite manufacturing

As can be seen from Figure 17, the curing cycle (applied after layup, vacuum bagging and storage in freezer) consisted of an initial ramp to 100 °C and held there for a relatively longer time to increase the resin flow and releasing the trapped air. Temperature increases to 150 °C with the same heating rate (5°C/min), and being held there to start the crosslinking reactions of the vitrimer resin and providing curing throghout whole resin. Finally, system ramps to 180 °C which is around the glass transition temperature of vitrimer matrix as mentioned, and being kept at this temperature to maximize the viscosity and complete the curing. After curing, controlled cooling again with 5°C/min cooling rate aims to minimize thermal stresses and avoid microcracking and minimize internal stress due to fast cooling

3.3. Vitrimer Matrix Composite Characterization

After completing the characterization of the vitrimer matrix and producing the initial composite samples via hand lay-up, testing and analysis of the vitrimer matrix carbon fiber composites begun. The first stage involved thermal analysis to investigate the influence of the vitrimer

matrix and its covalent adaptable network structure on the composite's behavior. This was followed by stress relaxation experiments, aiming to observe how the vitrimer's dynamic bonds respond to internal stresses developed during curing. Additionally, impedancemetry tests were conducted to examine the composite's electrical response and to identify potential critical phase transitions within the vitrimer matrix.

3.3.1. Thermal Characterization

The produced vitrimer matrix composite sample was cured and then cut to suitable dimensions using a diamond cutter for DMA testing . The sample was heated from room temperature up to 270 °C at a rate of 5 °C/min, exceeding the maximum temperature applied in the earlier vitrimer matrix-only analysis. Notably, the first peak observed in previous tests— initially related to humidity and later reasoned to be due to lack of curing of vitrimer matrix—was not present in this test. This absence suggests that the curing process applied during composite fabrication may have completed any remaining crosslinking, thereby eliminating the earlier observed thermal event. To add, the frequency of the DMA testing was 1 Hz which gave the least disturbed result set and graphic. Dynamic displacement value was different from the analysis done on vitrimer matrix sample, which was a lower magnitude (around 1 µm) than the matrix samples which had more thickness.

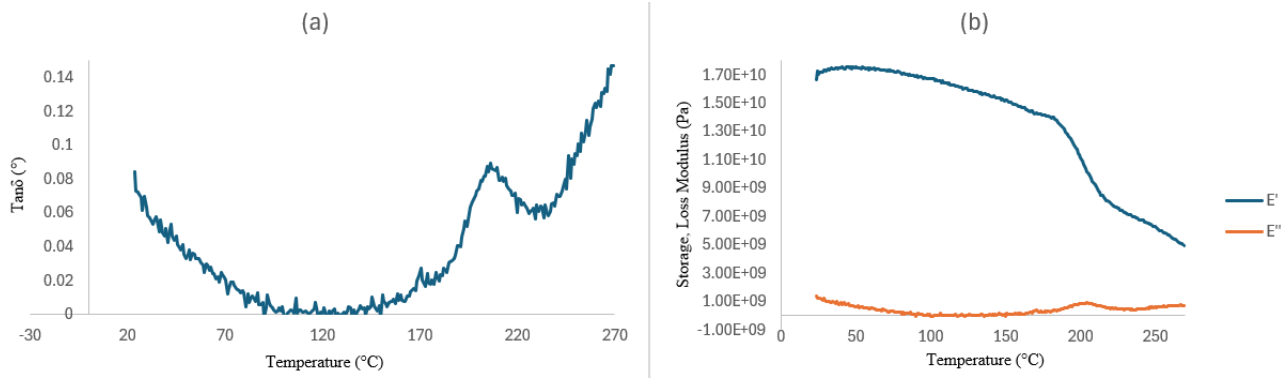

Figure 25 Tanδ, Storage Modulus and Loss Modulus versus Temperature graphs obtained from DMA analysis of vitrimer matrix composite

As seen from the DMA results in Figure 17, the degradation temperature was not reached, and therefore the expected secondary peak above the glass transition temperature (~190 °C) was not observed. However, the initial peak detected in the thermal characterization of the vitrimer matrix without fibers was also absent. This supports the theory that the vitrimer underwent additional curing during the composite fabrication process, eliminating any residual curing reactions that may have caused the first peak on the initial DMA study. It is also worth noting

that in composite systems, the secondary peak is often less pronounced or absent due to the constraint of fibers on the matrix. In this case, the constant drop in storage modulus at higher temperatures suggests that some network rearrangement or bond exchange activity may still be occurring, even though the full peak could not be captured within the tested temperature range.

3.3.2. Impedancemetry

Electrical impedancemetry is a non-destructive, real-time technique to monitor and characterize the curing process of polymer matrices. The methodology relies on the correlation between electrical properties, specifically impedance magnitude (|Z|) which is the material's resistance to the flow of alternating current and phase angle (θ) indicating the phase shift between the applied voltage and resulting current, temperature and time [26]. As curing progresses, changes in the polymer's molecular mobility and crosslink density are reflected in these electrical parameters. By evaluating both impedance and phase angle curves as well as their derivatives, it becomes possible to track the onset and progression of key polymerization transition phases such as PL (liquefaction), PG (gelation), PV (vitrification) and PF (final cure).

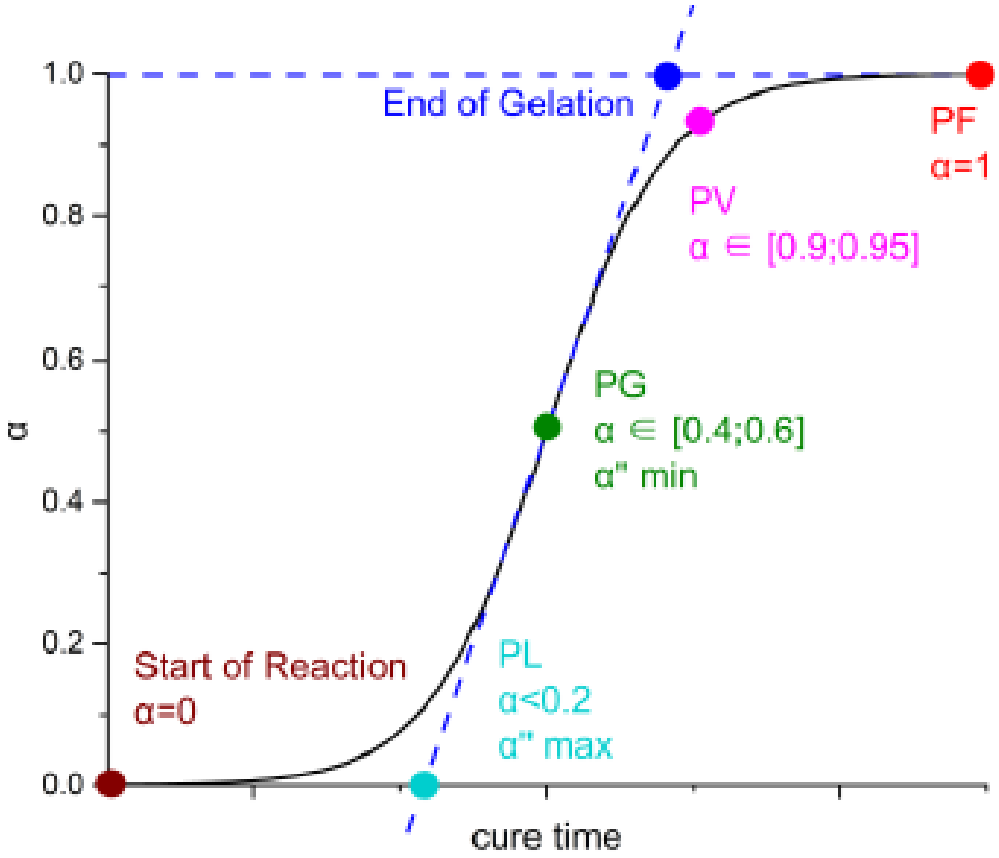

Figure 26 Example of identification of the critical physiochemical points of polymerization using the degree of curing [27]

A cure progression plot is given in Figure 18, where the degree of cure α(t) is used to define transitions in line with characteristic shifts in impedance and phase angle. The ability to detect these transitions electrically supports the development of intelligent process control systems in composite manufacturing which has the core principle of treating the material itself as a sensor by attaching electrodes to record electrical responses during curing. Furthermore, this method allows for the establishment of a direct correlation between electrical signatures and the degree of cure, which is typically calculated through kinetic modelling or differential scanning calorimetry (DSC) [28].

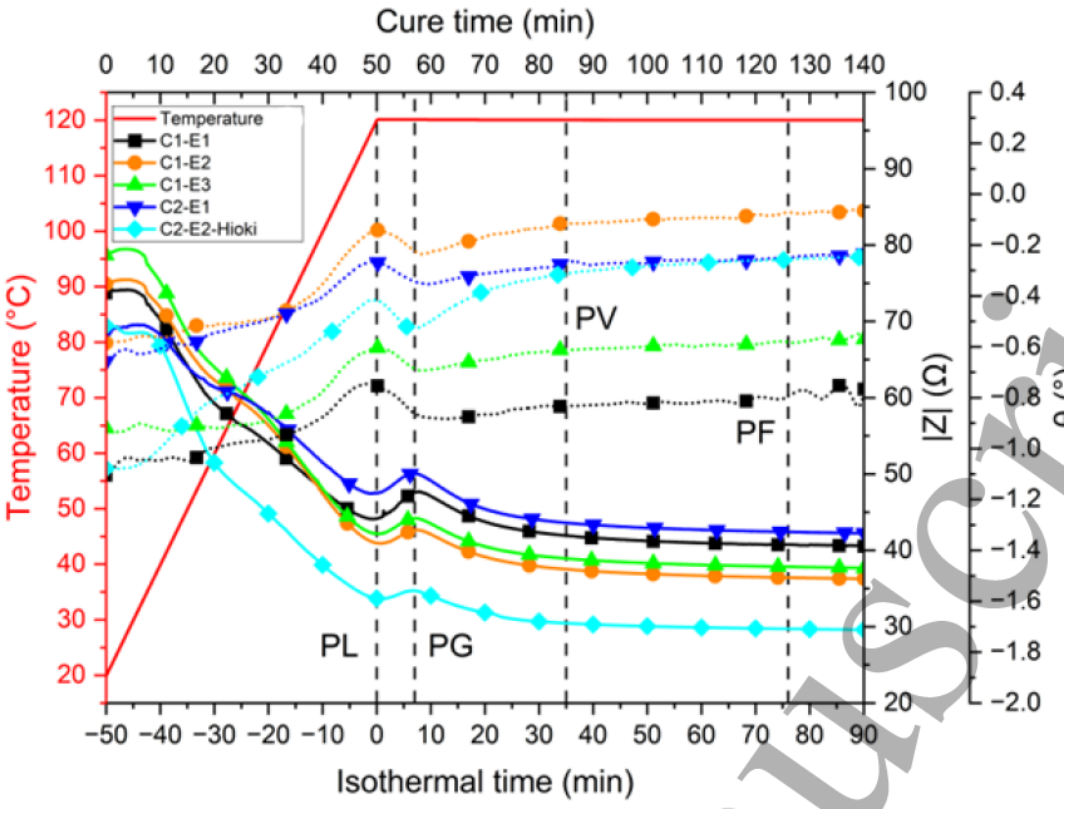

Figure 27 |Z| (solid lines) and θ (dashed lines) of [0°8] samples at10 kHz using the new homemade bench and Hioki impedance analyzer, for two different cure cycles denoted by C1 [27]

Figure 19 presents the evolution of impedance |Z| and phase angle θ over time during two different cure cycles (C1 and C2) for unidirectional vitrimer matrix composite samples. The curves highlight the correlation between electrical parameters and the critical curing stages of the composite matrix. Specific inflection points in the curves allow for the identification of key physico-chemical transitions such as PL (liquefaction), PG (gelation), PV (vitrification), and PF (final cure) likely to the analysis made by checking the curing degree. As observed, the drop in |Z| and the shift in phase angle align well with these curing transitions.

For the impedancemetry analysis conducted in this study, composite samples with a lay-up of $[0°]_8$ were prepared as previously described in the sample preparation section. Electrodes were positioned on the sample in three distinct configurations to capture measurements in the thorough-thickness, transverse, and diagonal directions. These electrodes were then connected to an impedance analyzer to monitor the electrical response of the composite throughout the curing process. As shown in Figure 20, the curing was carried out in a compression molding setup under applied pressure, following a predefined thermal cycle. The purpose of the setup was the real-time tracking of impedance (|Z|) and phase angle (θ) variations during the polymerization process, allowing identification of critical cure transition points in the composite

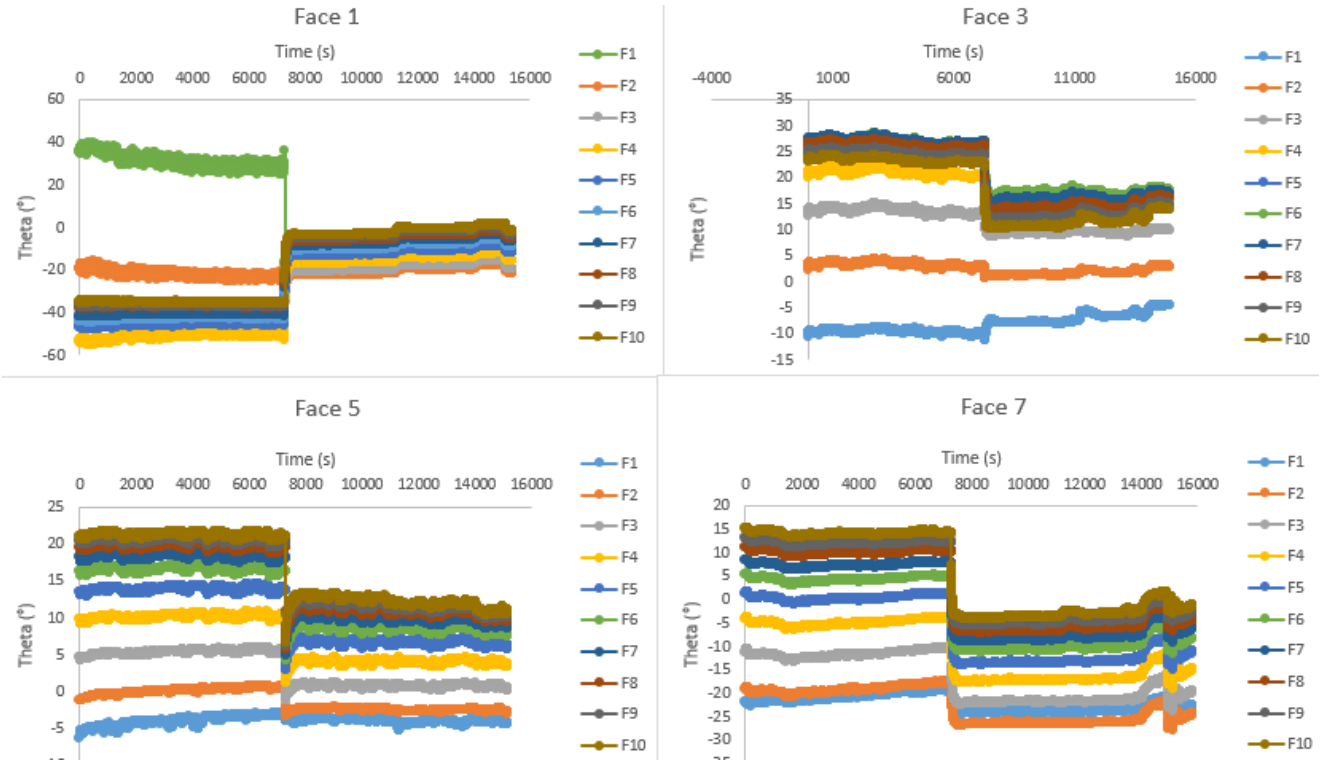

Figure 28 Phase angle-time results obtained for different faces from the initial impedancemetry test

As shown in Figure 21, a significant drop in phase angle (θ) is observed precisely at the moment when the composite sample was in concact to external pressure. This discontinuity is undesirable, as it introduces measurement noise and masks the intrinsic electrical behavior of the vitrimer composite. Based on this, the decision was made to eliminate applied pressure in future measurements to preserve the fidelity of the data. The results presented for each face include ten frequency values (F1 to F10), spanning from 5 kHz to 50 kHz. The variation in phase angle across frequencies suggests that the response of the composite is frequency-dependent, as expected.

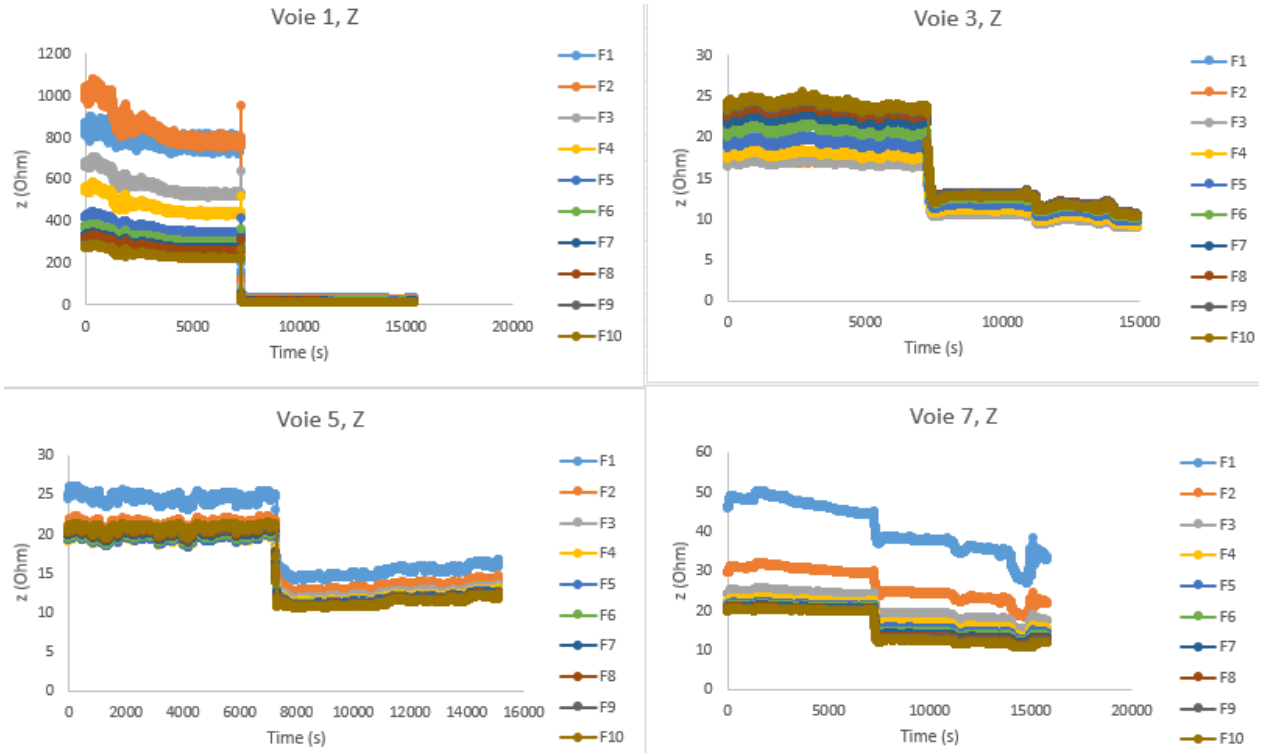

Figure 29 Impedance -time results obtained for different faces from the initial impedancemetry test

As observed in Figure 22, the impedance (Z) results exhibit a sharp drop at the moment external pressure is applied to the sample across all electrode configurations similarly to the phase angle results which confirms that the mechanical contact of this amount disturbs the electrical measurements by significantly reducing resistance values during curing. Differences in values between different faces and frequencies also confirms that the results obtained are frequency and ply orientation dependent.

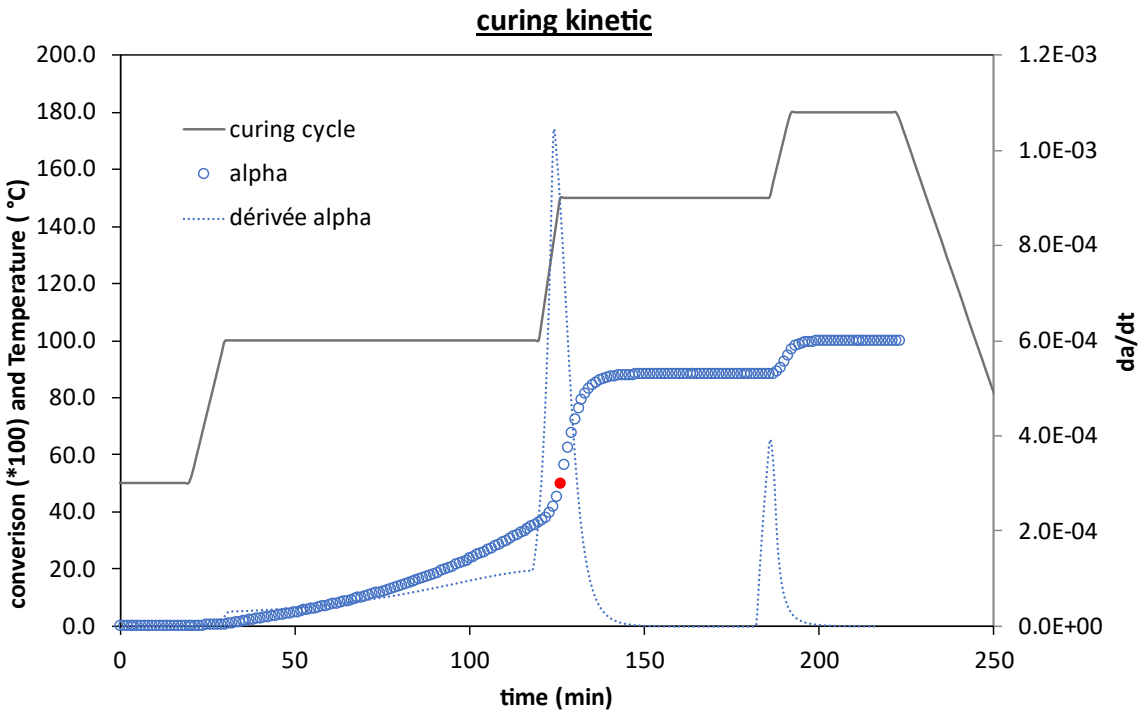

Figure 30 Curing kinetics and critical points received from impedancemetry

As shown in Figure 21, the gelation point (Pg) of the vitrimer matrix composite is reached at approximately 100 °C, with a corresponding curing degree of 0.506. To calculate the curing degree, Kamal Sourour and Di benedetto models were applied, making it able to calculate a precise curing degree at the gelation point. Following, the first vitrification point (Pv) is observed at around 150 °C, marking the transition where the resin mobility is reduced due to the formation of a strong crosslinked network. A second vitrification point is detected above 180 °C, which may be associated with the onset of dynamic bond exchange characteristic of the vitrimer matrix. Unlike conventional thermosets, this behavior suggests that bond rearrangement processes could be activated at elevated temperatures, potentially influencing the material's stress relaxation and post-curing characteristics.

However, as observed from the results presented in Figure Y ?? , the application of pressure during the compression molding process caused a significant drop in both impedance (|Z|) and phase angle (θ) values, indicating a disruption in the measurement. This anomaly is likely due to mechanical deformation affecting the electrode contact quality or introducing signal disturbances through pressure-induced damage to the connections. As a result, it was decided that upcoming impedance measurements would be conducted without applying pressure, to preserve signal clearness and obtain more reliable data during the curing cycle.

The initial impedancemetry analysis was carried out using a four-electrode configuration, with two electrodes placed on each side of the composite laminate, aligned in the same direction with the fibers. Four distinct sets of data were gathered based on electrode and wire positioning: Face 1 corresponded to the fiber direction on the top surface, Face 3 to the fiber direction on the opposite side, Face 5 to diagonally placed electrodes for off-axis measurements, and Face 7 to electrodes aligned transversely to the fibers. The frequency range used in these measurements was 5–50 kHz, which was selected based on preliminary tests conducted on uncured samples to identify the range that provided the clearest signal responses.

3.3.3. Stress Relaxation Behaviour

The initial samples prepared for stress relaxation measurements were cut to dimensions of 20 × 200 mm and consisted of biaxially reinforced laminates with a $[0/90]_2$ layup. The purpose of this configuration was to create internal stresses between differently oriented plies which were expected to create an amount of curvature after curing, enabling a clear observation of stress relaxation behavior during secondary thermal cycles with chemical mechanisms of vitrimer. Following curing, it was initially expected that the vitrimer-based samples would exhibit noticeable curvature due to internal residual stresses. This curvature was intended to serve as a baseline for conducting secondary thermal treatment, enabling observation of the vitrimers dynamic bond exchange mechanism and its role in stress relaxation which will be proved by a potential reduction in curvature upon reheating. However, contrary to expectations, the samples were taken from the oven nearly completely flat. This unexpected result caused the need for additional verification procedures to determine whether the vitrimers dynamic covalent network had already been activated during the initial curing process—potentially leading to stress relaxation and flatness—or if the outcome was due to issues related to hand lay-up manufacturing or experimental conditions (vacuum bag setup, oven conditions etc.).

Figure 31 First two biaxial samples after curing, completely flat and in contact with the surface

For further verification of the results of initial curing, two bimaterial samples were produced using the same hand lay-up procedure, this time combining vitrimer prepreg with aluminum, which were expected to induce more curvature after curing due to the mismatch in thermal

expansion coefficients between the two materials. The aluminum was cut in the sample dimensions and two layers of 90° vitrimer matrix prepreg material was layed up over the alumminum. Despite this, the aluminum–vitrimer composites also exited the oven without visible curvature.

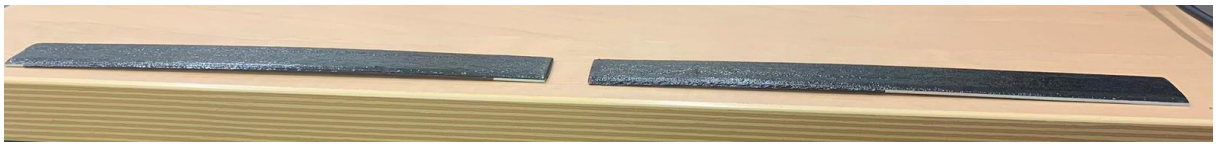

Figure 32 Bimaterial samples after curing

As a final step, reference epoxy-based biaxial laminates were fabricated using hand lay-up with manual fiber impregnation instead of using prepreg with the same fiber orientation, serving as a control group to validate whether the absence of curvature was unique to vitrimer behavior or due to a more general experimental issue. After curing, biaxial reference epoxy matrix samples were also flat as can be seen in Figure 25, which is completely unexpected since they do not possess the bond exchange mechanism characteristic of vitrimers. This outcome raised concerns that either a problem existed within the test setup itself or that the biaxial layup configuration was not generating sufficient internal stress to induce curvature.

Figure 33 Reference epoxy samples after curing

To verify the layup and verify that internal stress is created depending on the asymmetry, the biaxial $[0,90]_2$ vitrimer matrix sample was examined under optical microscopy to assess ply orientation accuracy and identify potential manufacturing defects. As seen in the cross-sectional images in Figure 26, the layered structure of the laminate is clearly distinguishable, validating the manual lay-up sequence. The fiber orientations alternate as expected, indicating the success of the biaxial stacking process.

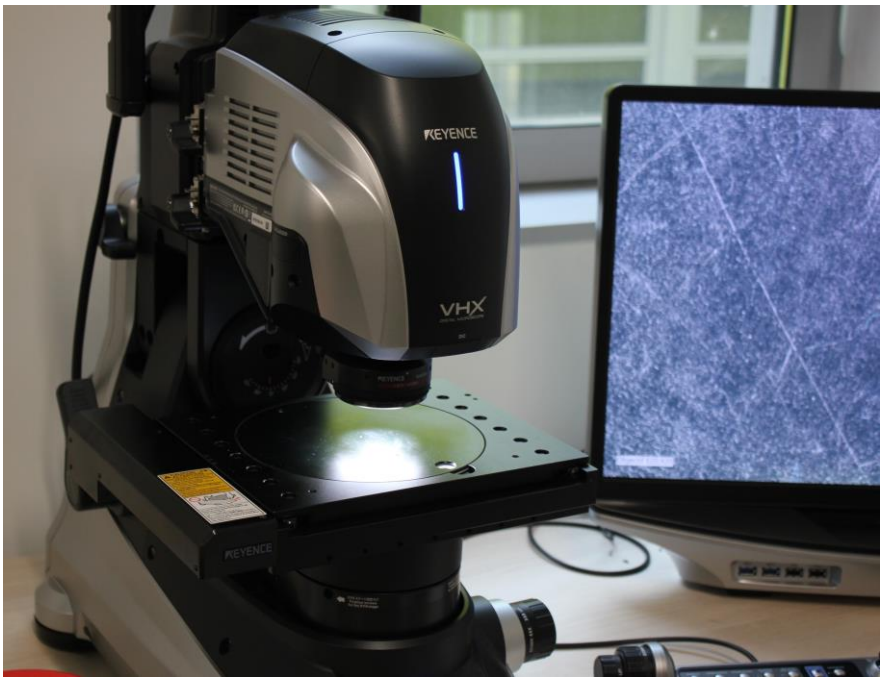

Figure 34 ~~SEM~~ equipment used for the photography (Keyence VHX 300)

The cross-sectional imaging of the biaxial laminates was performed using the Keyence VHX-3000 digital microscope which was photographed in Figure 31. This advanced microscope system allows for high-resolution imaging with a wide depth of field, enabling detailed analysis of surface features and microstructural properties. The instrument is equipped with a flexible observation system that supports both 2D and 3D imaging, making it usable for inspecting complex composite structures. The software also has the capability of accurate measurement and characterization of features within the laminates, allowing reliable observation of voids, defects, and fiber arrangements.

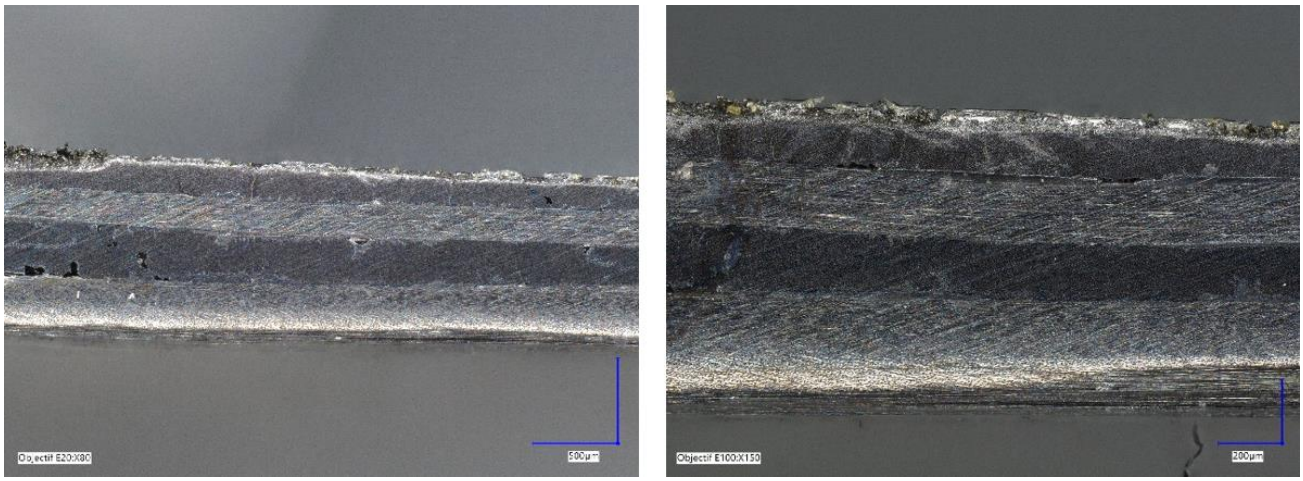

Figure 35 Microscopic images of biaxial composite sample ($[0,90]_2$: 500 µm, 200 µm)

A significant number of defects are visible across the laminate. These include porosities, both between the plies and within individual layers, likely caused by insufficient compaction created during the layup or incomplete air evacuation during the vacuum bagging process. In addition, interlaminar gaps and resin-rich pockets can be observed, suggesting uneven resin flow or pressure distribution during curing. The presence of voids and small cracks along the fiber-matrix interface further supports the need for improved processing control.

[POROSITY, VOID CALCULATION IMAGEJ]

After confirming that the layup had been correctly performed and that an actual asymmetry existed which was insufficient to generate significant internal stress, a series of modifications were made to both the layup configuration and the vacuum bagging setup. The original $[0,90]_2$ layup was replaced with a [0,90,0,90] configuration to increase the level of asymmetry and the created internal stress within the laminate. Additionally, the breather textile placed between the releasing agent and the steel mold in the initial vacuum bag setup was removed. Three new samples with the same dimensions were prepared and placed in the same vacuum bag for curing under the same conditions. For the first two, the samples were laid on a releasing agent, but with different outer ply orientations (0° and 90°) in contact with the steel mould to investigate the influence of ply direction in contact with steel mould on curvature formation. The third sample was positioned on top of a breather textile, replicating the earlier setup, to determine whether the breather layer had been preventing the curvature in previous tests.

Figure 36 Samples with curvature after curing (a) 0 degree ply in direct contact with mold, (b) 90 degree ply in direct contact with mold, (c) contact with the mold over breather textile

As shown in Figure 27, all three samples exhibited noticeable curvature upon removal from the oven after curing. This outcome eliminates the breather textile as a contributing factor in the absence of curvature in the first sets of experiments, since the third sample which is prepared with the breather textile beneath it also developed a curvature. Instead, the results support the assumption that the initial $[0,90]_2$ layup lacked sufficient internal stress to trigger deformation. Additionally, all three samples had a curvature in the direction of the 0° ply, regardless of which

ply faced the steel mould. This suggests that the 0° orientation is the dominant stress-concentrating layer and primarily decides the direction of curvature.

A calculation of curvature was performed for the three asymmetric laminate samples using their measured geometry, following the method described by Arao et al. (2010). The analysis uses the laminate's chord length and the vertical distance between the mid-plane and the outer surface to determine the curvature radius (ρ) of each sample.

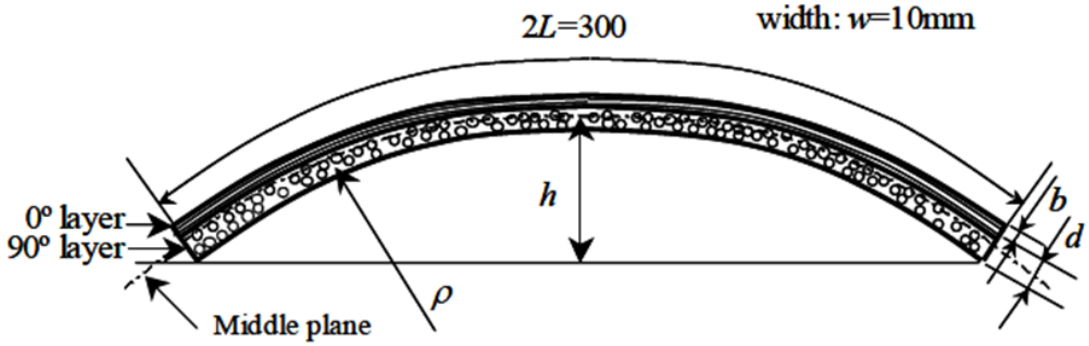

Figure 37 Size and geometry of unsymmetric laminate [29]

The formula shown below was used to calculate the curvature radius (ρ) of the samples, based on the measured arc height (h) and half-length (L) of the curved laminate sections

$$h^2 - 2h\rho + \rho^2 \sin^2\left(\frac{L}{\rho}\right) = 0 \text{ (Eq 1.1) [30]}$$

As summarized in Table 5, the sample placed with the 0° ply facing the steel mould showed the largest curvature (highest ρ), indicating more internal stress accumulation in that configuration. The sample placed with the 90° ply facing the mould had slightly less curvature, suggesting that the orientation of the outermost ply does influence stress development during curing. The sample cured over the breather textile exhibited the smallest radius (least curvature), which reinforces the idea that the presence of a breather textile reduced residual stress by also reducing the difference in thermal expansion coefficient between the sample and the mold.

Table 5 Samples with contact surfaces, dimensions and calculated curvature radius

Sample (contact surface)	L (mm)	h (mm)	Curvature radius (ρ)
s1 (releasing agent, 0)	100	6	18.35
s2 (releasing agent, 90)	100	5.2	18.16
s3 (textile, 0)	100	4	17.86

It is noteworthy that both samples without breather textile, despite being placed on the mould with different ply orientations in contact (one with the 0° plies facing the mould and the other with the 90° plies), showed curvature in the same direction. In both cases, the curved surface was located on the 0° ply side, indicating that this fiber direction is the primary stress concentrator within the composite.

3.3.4. Post Curing Experiments

After the initial curing process was completed and the composite samples exhibited measurable curvature, the curvature radius of each sample was calculated and building on the results, a secondary curing process was undertaken to further investigate the thermo-mechanical behavior of the vitrimer matrix. This step aimed to observe whether the vitrimer's dynamic bond exchange mechanisms could be activated under additional thermal cycling, allowing internal stresses to be released. For this purpose, the curved samples were subjected to an additional controlled heating and cooling cycle in an oven, following a similar thermal profile to the initial cure but without the application of external load or pressure. The hypothesis was that, if the vitrimer network retained bond exchange capability at elevated temperatures, the polymer chains could rearrange and relieve residual stresses, thereby reducing or eliminating the curvature.

This post-curing experiment was carried out on the two composite samples that exhibited the highest curvature from the initial curing stage (the ones without breather textile) with 0° and 90° plies in contact with the mould surface. The purpose of the experiment was to monitor curvature change in real time under thermal conditions that could potentially activate vitrimer bond exchange. To achieve this, the oven used for post-curing, which featured a glass viewing window, was fitted with a camera setup positioned directly in front to capture images of the samples every five minutes throughout both heating and cooling stages. Inside the oven, a simple observation rig was constructed consisting of a flat support surface covered with breather textile to increase the color contrast, and a fixed ruler placed adjacent to the samples to serve as a scale reference in the photographs. Additionally, a thermostat was attached to the sample to provide accurate real-time tracking of the temperature. The samples were heated to just above 180 °C but kept below 200 °C to avoid matrix degradation, and held at this elevated temperature for approximately 45 minutes. This hold stage was chosen to allow sufficient time for the vitrimer's dynamic covalent bonds to perform exchange reactions, enabling relaxation of internal residual stresses. During the entire process, both the temperature profile and the

physical state of the samples were monitored through continuous photography of the scale for the height, enabling correlation between the thermal cycle and any observable reduction in curvature.

The first sample subjected to secondary curing was the one with 0° plies in contact with the mould, which had shown the highest initial curvature. As seen in Figure 29, the sample's height which is used as an indicator of curvature decreased steadily as temperature increased. Notably, the curvature began reducing significantly even before reaching the glass transition temperature (~150 °C) and reached zero just prior to that point, indicating that stress relaxation mechanisms were already being activated at lower temperatures. During the hold stage at the glass transition range, no curvature was observed, suggesting that the stored internal stresses were fully relieved. However, upon cooling, a small amount of curvature reappeared, showing that some residual stresses returned after cooling. Despite this partial recovery, the final curvature height was substantially lower than the initial value, confirming that secondary curing effectively reduced the stress in the vitrimer composite.

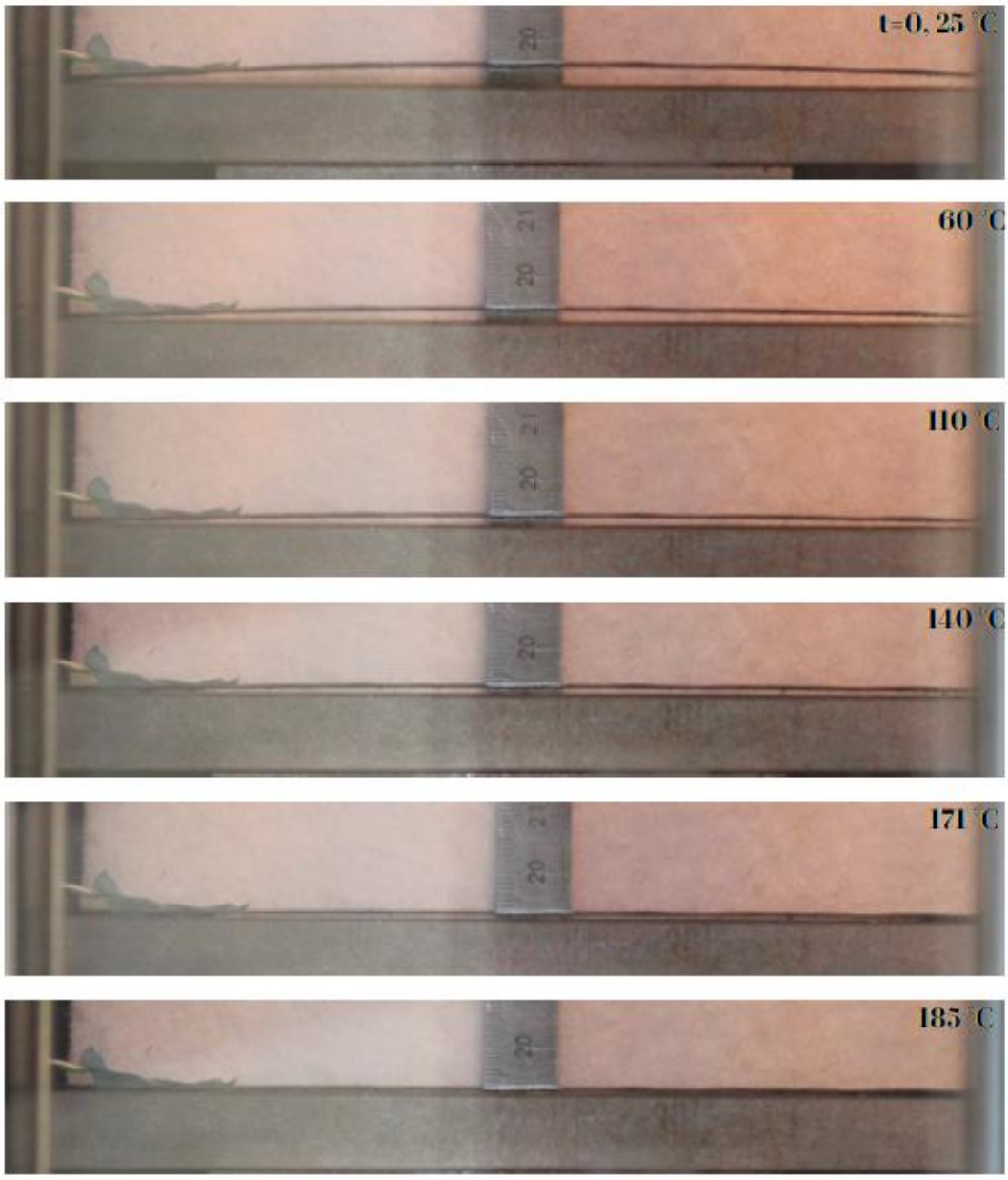

Figure 38 Photography and change in curvature during the heating of the first sample (cured with a contact between 0° ply and the mold)

Figure 29 shows the progressive reduction of curvature during the heating phase of the post-curing process for the vitrimer composite, as it is raised to temperatures approaching the glass transition range. Initially, the sample (cured with a contact between 0° ply and the mold) had a curvature of nearly 6 mm, but this gradually diminished with increasing temperature. By the time period the vitrimer matrix composite reached the glass transition temperature (Tg), the curvature had completely reduced to zero. This behavior indicates that the internal stresses responsible for the deformation were effectively relieved before and during the Tg region. The observation supports the hypothesis that stress relaxation in such materials can occur well

before degradation temperatures are approached, enabling shape recovery without compromising structural integrity.

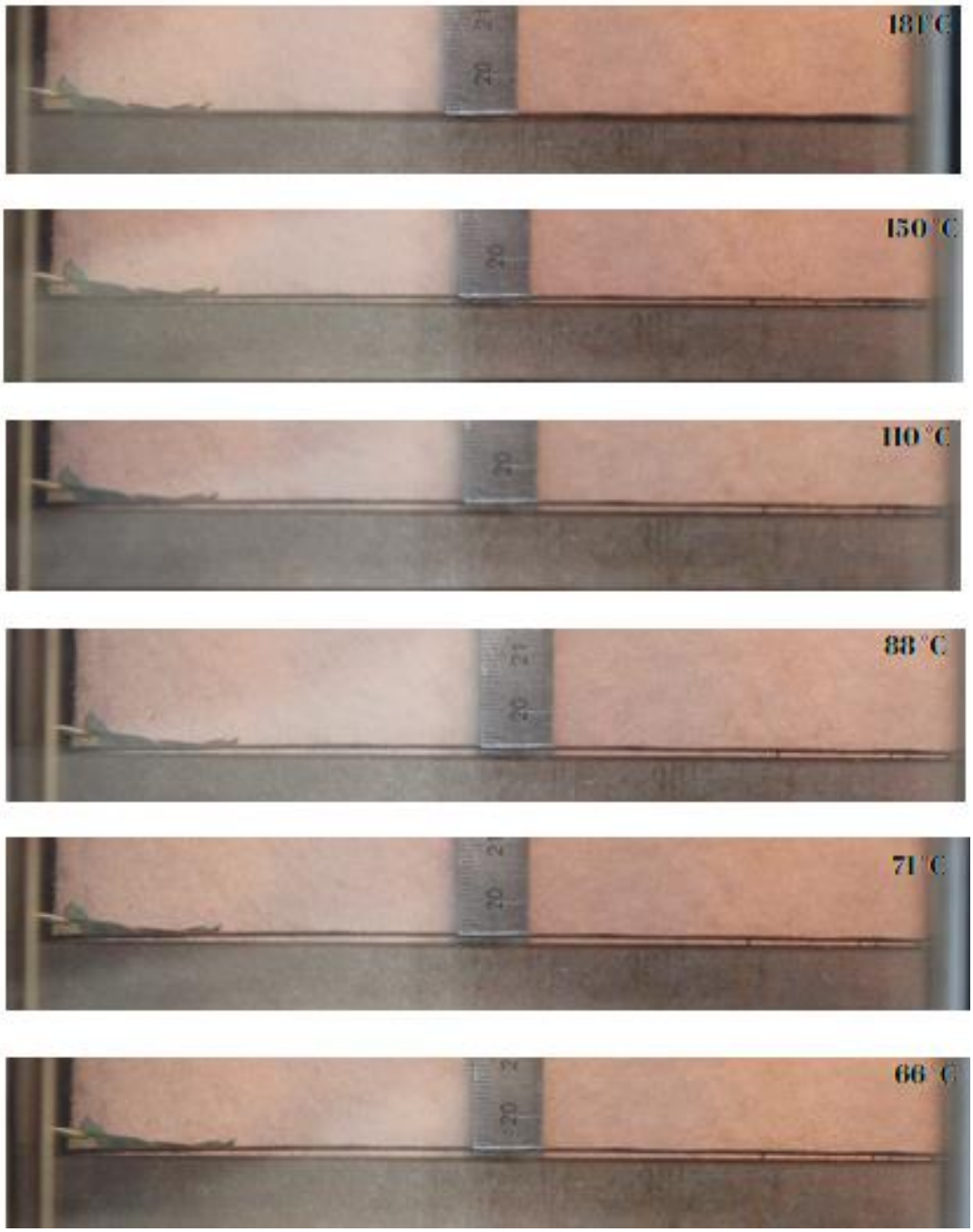

Figure 39 Photography and change in curvature during the cooling of the first sample (cured with a contact between 0° ply and the mold)

Figure 30 presents the sequence of photographs taken during the cooling phase of the post-curing process for the vitrimer composite sample with the 0° ply in direct contact with the mold. Cooling was conducted from the glass transition temperature range down to slightly above room temperature. The curvature which had originally reduced to zero during heating decreased to a

lower value than its initial pre-heating value at the end of the cycle. This observation shows that a portion of the residual stress was relieved during the process. While it cannot be stated with certainty whether this stress relaxation was primarily driven by the vitrimer matrix's dynamic bond exchange mechanisms or a more conventional thermoset stress relaxation behavior, the results strongly suggest a stress-release phenomenon influenced by the vitrimer's adaptable network.

Also, it is possible to achieve relax more internal stresses, the exposure time within the glass transition range or the peak temperature (while remaining below 200 °C to avoid material degradation) might be increased. A longer hold at these conditions could more effectively activate the covalent adaptable network and increase the amount of dynamic bond exchange reactions within the vitrimer matrix, thereby enabling further stress relaxation and more curvature reducing.

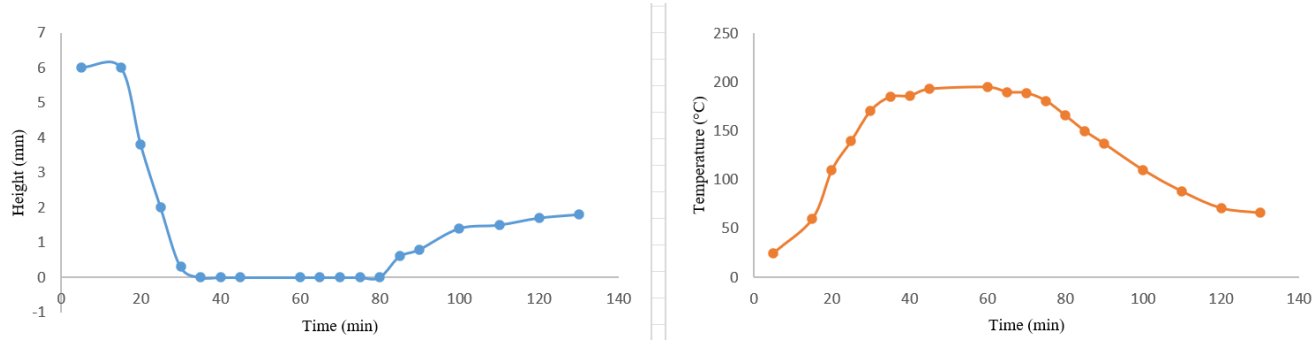

Figure 40 Height (proportional to curvature) and temperature versus time for the first sample

The graphs on Figure 31 show that the sample's initial center height from the surface was about 6 mm at room temperature before post-curing. As the temperature increased and the sample was held in the glass transition region (just below 200 °C to avoid degradation) for about an hour, the curvature decreased rapidly, reaching to 0 before Tg. During the glass transition hold, the height (curvature) stayed at zero which means a full stress relaxation at viscous phase. Upon cooling, a slight curvature (about 2 mm) reappeared, indicating partial recovery of residual stresses, but the final curvature was still significantly lower than the initial state. This behavior suggests that post-curing allowed for substantial stress relaxation, potentially due to vitrimer matrix dynamics such as covalent adaptable network activation and bond exchange reactions—though the partial return of curvature implies that longer or slightly higher-temperature holds (without exceeding 200 °C) might be required for complete stress relaxation.

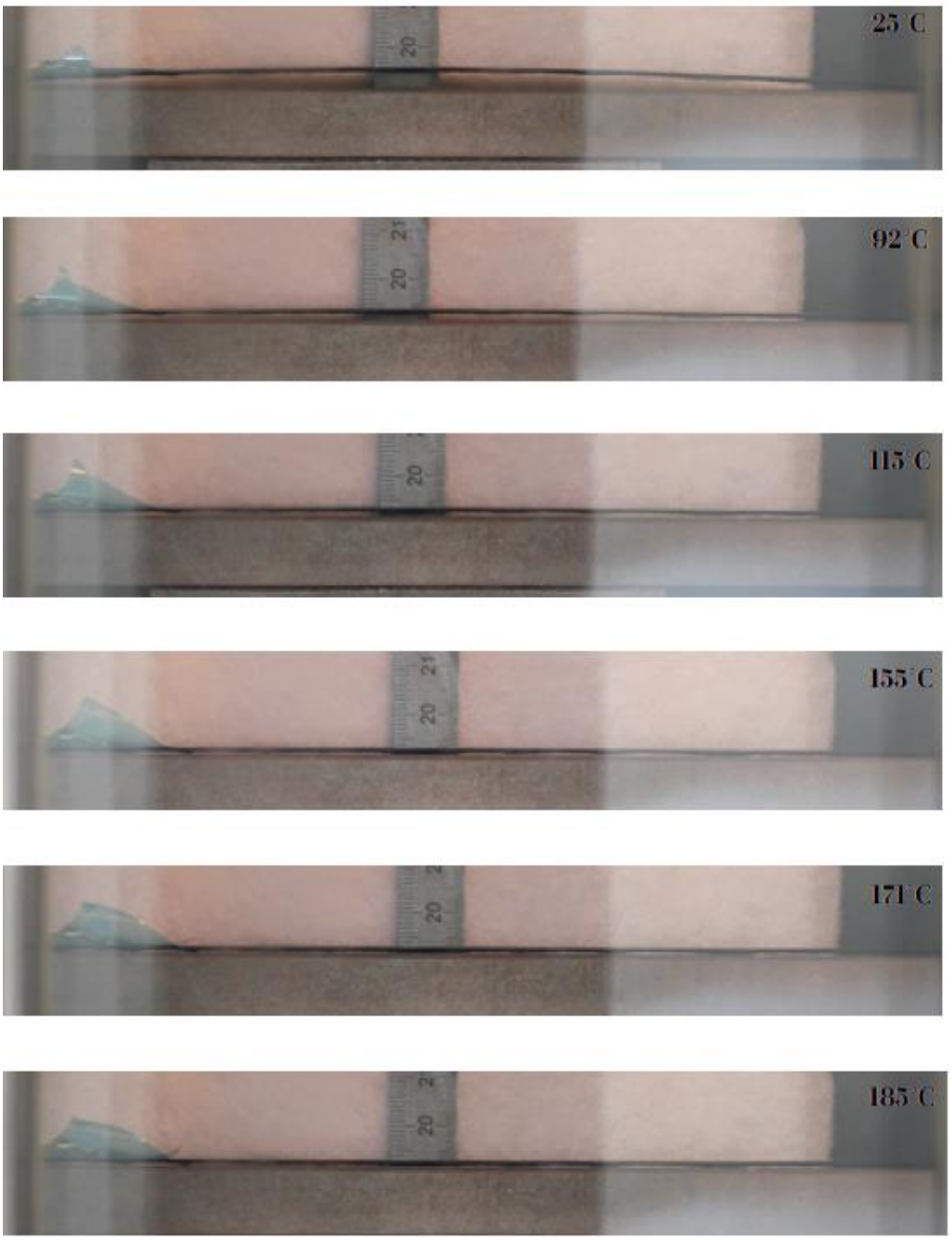

Figure 41 Photography and change in curvature during the heating of the second sample (cured with a contact between 90° ply and the mold)

For the second sample (90° ply in direct contact with the mould), the heating cycle created a very similar curvature evolution to the first sample. The initial curvature was slightly less than that of the 0° ply-contact sample, but the trend was consistent: the curvature progressively decreased during heating and reached zero before the glass transition temperature (Tg) was attained. This suggests that the stress relaxation process—potentially linked to the vitrimer's dynamic bond exchange—was already substantially active before Tg, at least under the tested heating conditions. The only minor difference observed was that for this sample, the point of

zero curvature occurred slightly closer to the Tg range compared to the first sample. This further supports the idea that ply orientation and contact surface with the mould may slightly influence the stress relaxation kinetics, but the overall mechanism remains similar.

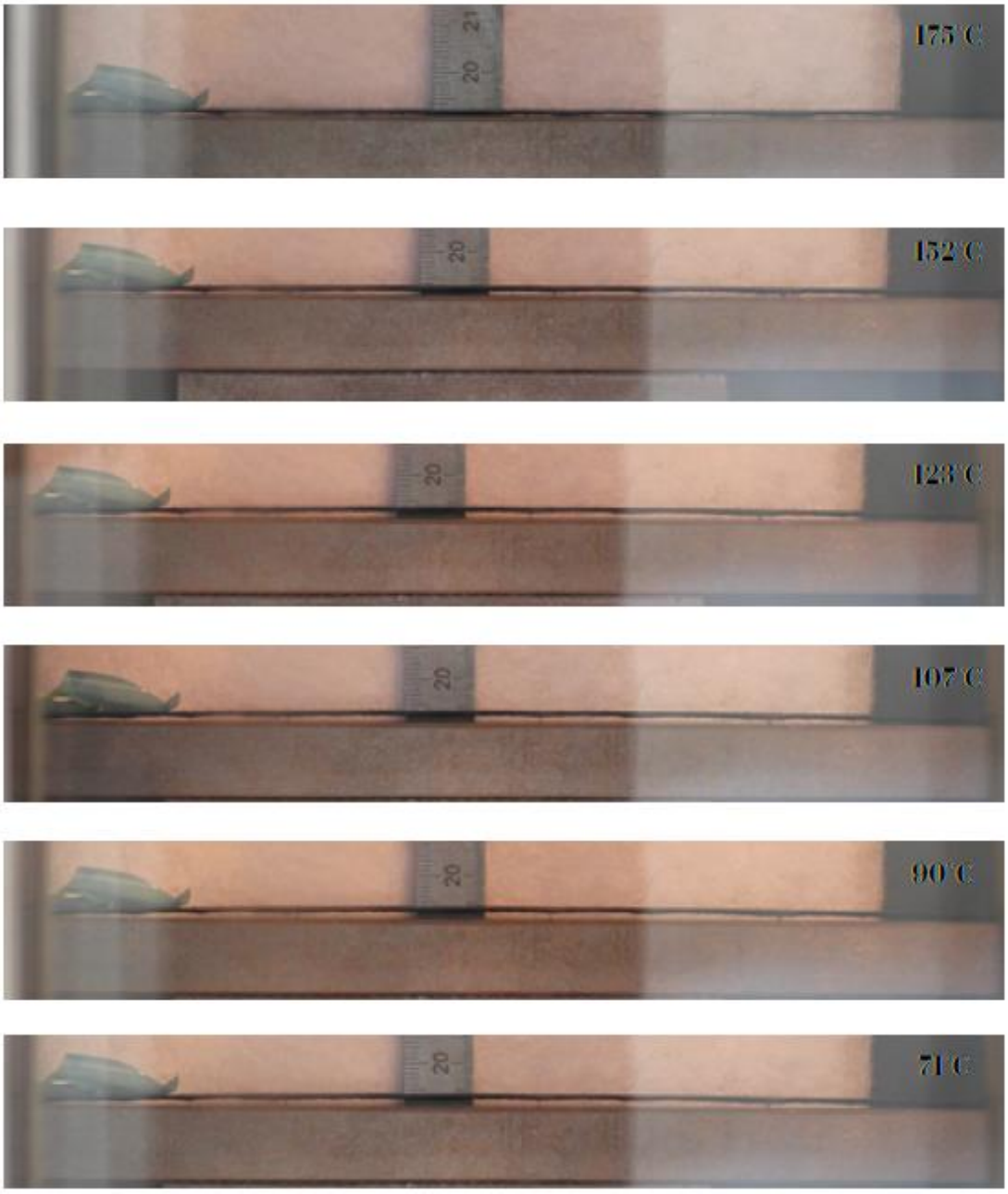

Figure 42 Photography and change in curvature during the cooling of the second sample (cured with a contact between 90° ply and the mold)

The photographic sequence on Figure 33 shows the cooling phase of post-curing for the second sample. In this case, the composite had the 90° ply in direct contact with the mold. Compared to the first sample, the final curvature at the end of cooling was noticeably lower, indicating that more internal stress was relaxed during the process. The likely reason for this is that the sample remained in the glass transition temperature range for approximately thirty minutes

longer than the first one, allowing more time for stress relaxation mechanisms to occur. Additionally, the initial curvature of this second sample before heating was already a little bit smaller than that of the first sample, which may have also contributed to the reduced final curvature observed after cooling.

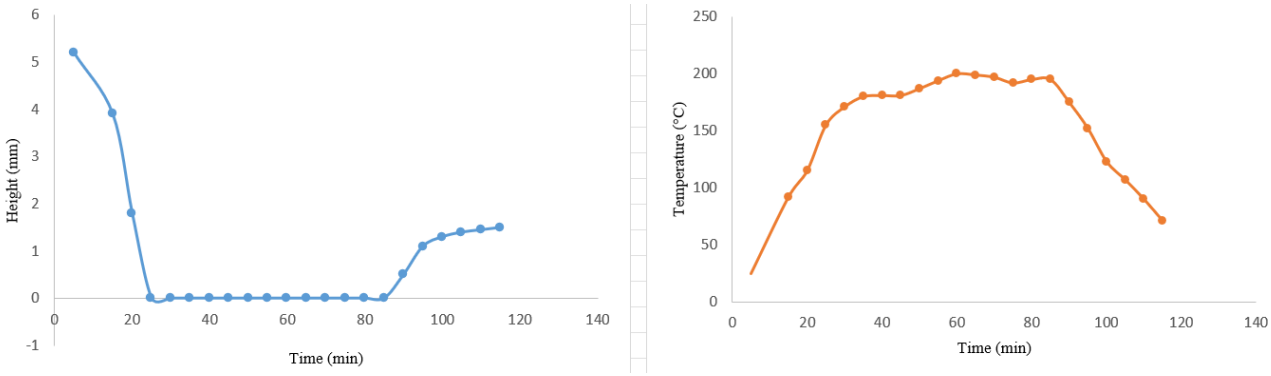

Figure 43 Height (proportional to curvature) and temperature versus time for the second sample

Figure 34 shows the height (which is proportional to curvature) and temperature versus time profiles for the second sample during the post-curing process. The initial height from the surface (representing the starting curvature) was already lower compared to the first sample, indicating less initial residual stress to be relaxed. Throughout the heating stage, the curvature decreased in the same behavior with the first sample but at the end, the reduction ratio in curvature was more. This more decrease is related to the fact that the second sample was maintained in the glass transition temperature range for approximately thirty minutes longer. This extended hold might have allowed additional time for the vitrimer matrix to undergo stress relaxation in its viscous state, likely caused by the dynamic bond exchange processes inherent to covalent adaptable networks. As a result, the final curvature after cooling was significantly lower than in the first sample, demonstrating that prolonged exposure within the glass transition range can enhance stress release and reduce final deformation.

THIS PAGE WAS INTENTIONALLY LEFT BLANK

4. CONCLUSION

5. FUTURE WORK

[1] ISMAIL, S. IK IR U. O. LU WA RO TI MI. “Recycling of Composite Materials.” Advances in Machining of Composite Materials, Springer International Publishing, 2021.

[2] H. Chalaye, Composite materials: drive and innovation. Le 4 Pages, des statistiques industrielles, No. 158 – February 2002. Available from

[2] Oliveux, G.; Dandy, L.O.; Leeke, G.A. Current status of recycling of fibre reinforced polymers: Review of technologies, reuse and resulting properties. Prog. Mater. Sci. 2015,72, 61–99

[3] The International Air Transport Association (IATA). Helping Aircraft Decommissioning. 2020. Available online: https://www.iata.org/en/programs/environment/aircraft-decommissioning/ (accessed on 17 December 2020)

[4] Krauklis, Andrejs & Karl, Christian & Gagani, Abedin & Jørgensen, Jens. (2020). Composite Material Recycling Technology – State-of-the-Art and Sustainable Development for the 2020’s

[5] Amaechi, C.V.; Agbomerie, C.O.; Orok, E.O.; Ye, J. Economic Aspects of Fiber Reinforced Polymer Composite Recycling. In Encyclopedia of Renewable and Sustainable Materials; Elsevier BV: Oxford, UK, 2020; pp. 377–397

[6] J.M Henshaw, W. Han, A.D. Owens, An overview of recycling issues for composite materials, Journal of Thermoplastic Composite Materials 9

[7] J.M. Henshaw, Recycling and disposal of polymer–matrix composites, in: D.B. Miracle, S.L. Donaldson (Eds.), ASM Handbook, Volume 21: Composites, ASM International®, 2001, pp. 1006–1012.

[1] Bergström, J. (2015) Mechanics of Solid Polymers: Theory and Computational Modeling. Mechanics of Solid Polymers: Theory and Computational Modeling. 1-509

[2] Karuppiah A. (2016) Predicting the Influence of Weave Architecture on the Stress Relaxation Behavior of Woven Composite Using Finite Element Based Micromechanics

[3] Manaia J.P., Manaia A.T.& Rodriges L. (2019) Industrial Hemp Fibers: An Overview. Fibers, 7 (106)

[4] Nordin N., Salleh Z., Kasolang S.& Ahmad M.A. (2013) Wear Rate of Natural Fibre: Long Kenaf Composite. Procedia Engineering, 68

[5] Denissen W., Winne J.M. & Prez F.E (2016) Vitrimers: Permanent Organic Networks with Glass-like Fluidity. Chemical Science 7 (1)

[6] Luzuriaga A.R., Martin R., Markaide N., Rekondo A., Cabanero G., Rodriguez J.& Odriozola I. (2016) Epoxy Resin with Exchangeable Disulfide Crosslinks to Obtain

Reprocessable, Repairable and Recyclable Fiber-Reinforced Thermoset Composites. Material Horizons 3, 241-247

[7] Schenk V., D'Elia R., Olivier P., Lebastie K., Destarac M.& Guerre M. (2023) Exploring the Limits of High-Tg Epoxy Vitrimers Produced through Resin-Transfer Molding. ACS Applied Materials & Interfaces 15 (39)

[8] Weidmann S., Volk P., Mitschang P.& Markaide N. (2022) Investigations on Thermoforming of Carbon Fiber Reinforced Epoxy Vitrimer Composites. Composites: Part A 154

[9] Kloxin C.J.& Bowman C.N. (2013) Covalent Adaptable Networks: Smart, Reconfigurable and Responsive Network Systems. Chemical Society Reviews 42 (17), 7161-7173

[10] Perna A.S., Astarita A., Martone A.& Palmieri B. (2025) Investigating the Feasibility of Metallizing Reprocessable Vitrimeric Components through Cold Spray Technique. Journal of Materials Engineering and Performance

[11] Luzuriaga A.R., Markaide N., Salaberria A.M., Azcune I., Rekondo A.& Grande H.J. (2022) Aero Grade Epoxy Vitrimer Towards Commercialization. Polymers 14 (15), 3180

[12] Yang Y., Xu Y., Ji Y.& Wei Y. (2021) Functional Epoxy Vitrimers and Composites. Progress in Material Science 120

[13] Schenk V., Labastie K., Destarac M., Olivier P., Guerre M. (2022) Vitrimer Composites: Current Status and Future Challenges. Materials Advances 3, 8012.

[14] Hafeezullah M., Wei Y., Zhang L., Jiang Q.& Liu W. (2020) An Imine-Containing Epoxy Vitrimer with Versatile Recyclability and Its Application in Fully Recyclable Carbon Fiber Reinforced Composites. Composites Science and Technology. 199.

[15] Oliveira I., Sandro A., Souza A.& Antonio L. (2013). Resin transfer molding process: A Numerical and Experimental Investigation. The International Journal of Multiphysics. 7, 125-136.

[16] Vincent Schenk, Philippe Olivier, Karine Labastie, Mathias Destarac, Marc Guerre, Carbon fibres/RTM6 vitrimer and non-dynamic epoxy thermoset composites: comparative study of manufacturing, mechanical characteristics, water absorption, impact resistance, repairing and compression after impact, Composites Part B: Engineering, 304

[17] Vincent Schenk, Joséphine de Calbiac, Raffaele D'Elia, Philippe Olivier, Karine Labastie, et al.. Epoxy Vitrimer Formulation for Resin Transfer Molding: Reactivity, Process, and Material Characterization. ACS Applied Polymer Materials, 2024, 6 (10), pp.6087-6095.

[18] Martinez, P.; Nutt, S. Flax–Reinforced Vitrimer Epoxy Composites Produced via RTM. J. Compos. Sci. 2024, 8, 275.

[19] Luthada, Pravin. (2022). The Introduction to the Filament Winding Process.

[20] Alms, J., Sambale, A. K., Fuchs, J., Lorenz, N., von den Berg, N., Conen, T., Çelik, H., Dahlmann, R., Hopmann, C., & Stommel, M. (2025). Qualification of the Vitrimeric Matrices in Industrial-Scale Wet Filament Winding Processes for Type-4 Pressure Vessels. Polymers, 17(9), 1146

[21] Lorenz N, Zawadzki T, Keller L, Fuchs J, Fischer K, Hopmann C. Characterization and modeling of an epoxy vitrimer based on disulfide exchange for wet filament winding applications. Polym Eng Sci. 2024;1-21

[22] Middleton B. (2016) Composites: Manufacture and Application, Design and Manufacture of Plastic Components for Multifunctionality. William Andrew Publishing, p. 53-101

[23] Bilal, Muhammad. (2022). COMPOSITE FORMATION BY HAND-LAYUP PROCESS.

[23] Zin, Mohd & Razzi, M & Othman, S & Liew, Kan-Ern & Abdan, K & Mazlan, Norkhairunnisa. (2016). A review on the fabrication method of bio-sourced hybrid composites for aerospace and automotive applications. IOP Conference Series: Materials Science and Engineering. 152. 012041. 10.1088/1757-899X/152/1/012041.

[24] Kevin M.& Noah M. (2020) Dynamic Mechanical Analysis. 10.1201/9780429190308.

[25] Jones S.D. (1999) Dynamic Mechanical Analysis of Polymeric Systems of Pharmaceutical and Biomedical Significance. International Journal of Pharmaceutics 179 (2), 167-178

[26] Andrzej L. (2014) Electrochemical Impedance Spectroscopy and It's Applications, Definition of Impedance on Electrical Circuits. 2, 7-66

[27] Bao H., Marguerès P.& Olivier P. (2024) An Innovative and Low-cost System for In Situ and Real-time Cure Monitoring Using Electrical Impedancemetry for Thermoset and CFRP Laminate. Measurement Science and Technology 35 (3)

[28] Han Y., Wang J., Zhang H., Zhao S., Ma Q.& Wang Z. (2016) Electrochemical Impedance Spectroscopy (EIS): An Efficiency Method to Monitor Resin Curing Processes. Sensors and Actuators A: Physical 250, 78-86

[29] Arao, Yoshihiko & Koyanagi, Jun & Okudoi, Yukie & Otsuka, Masanori & Kawada, Hiroyuki. (2010). Residual Stress Relaxation in CFRP Cross-ply Laminate. Journal of Solid Mechanics and Materials Engineering. 4. 1595-1604. 10.1299/jmmp.4.1595.

[30] Nairn, J.A., Zoller, P. Matrix solidification and the resulting residual thermal stresses in composites. J Mater Sci 20, 355–367 (1985). https://doi.org/10.1007/BF00555929